Automated Container Transport System between Inland Port and Terminals

Principal Investigators:

Petros Ioannou

University of Southern California
Center for Advanced Transportation Technologies
EE-Systems, EEB200, MC2562
Los Angeles, CA. 90274

Anastasios Chassiakos

California State University
College of Engineering
Long Beach, CA. 90840-5602

Graduate Students:

Jianlong Zhang
Alexander Kanaris
Ricardo Unglaub

December 2002

DISCLAIMER

The contents of this report reflect the views of the authors, who are responsible for the facts and the accuracy of the information presented herein. This document is disseminated under the sponsorship of the Department of Transportation, University Transportation Centers Program, and California Department of Transportation in the interest of information exchange. The U.S. Government and California Department of Transportation assume no liability for the contents or use thereof. The contents do not necessarily reflect the official views or policies of the State of California or the Department of Transportation. This report does not constitute a standard, specification, or regulation.

ABSTRACT

Due to the fast growing rate of the global container trade, every major port is under the pressure of meeting the projected capacity demand. The scarcity of land at ports in many Metropolitan areas makes it difficult if at all possible to improve capacity by expanding the terminal area. As a result alternative solutions have been sought for improving capacity and meeting the growing demand for container storage area and terminal capacity.

In this study we propose a new concept called "Automated Cargo Transportation system between Inland POrt and Terminals" (ACTIPOT) which involves the use of automated trucks to transfer containers from an inland port to terminals. The inland port could be a few or more miles away from the terminals where lower cost land is available and is used for storing and processing import/export containers before distribution to customers or transfer to the terminal for loading on ships.

In this report, we design, analyze, simulate and evaluate the various components of the ACTIPOT system with emphasis on the lateral and longitudinal control of the automated trucks and on the overall supervisory controller that synchronizes all operations and transfer of containers between the terminal and inland port using dedicated truck lanes. We employ the use of truck platoons in order to make the control of the overall system easier to handle and understand therefore minimizing the possibility of deadlocks, congestion and failures. Simulations are used to demonstrate that each subsystem operates in a satisfactory manner. Larger scale microscopic simulations are performed to demonstrate the overall performance of the ACTIPOT system. The choice of distances and other variables in the ACTIPOT system are selected by using the ICTF facility as the inland port and Pier G as the terminal both located in the Long Beach area.

TABLE OF CONTENTS

LIST OF FIGURES

1 INTRODUCTION

In recent years, the global container trade has been growing at an annual rate of about 9 percent, and the corresponding U.S. rate has been around 6 percent. By 2010, it is expected that 90 percent of all liner freight will be shipped in containers. Thus every major port is expected to double or even triple its processed containers by 2020 [2]. In order to remain competitive, marine container terminals in metropolitan areas must meet the increasing demand for storage and processing capacity. Ports such as those of Los Angeles/Long Beach (LA/LB), which handle nearly one third of all U.S. foreign container traffic, are under a lot of pressure to meet projected capacity demand increases in order to remain competitive and avoid congestion at the terminals and contiguous areas. One feasible approach to reduce the pressure of increased storage capacity demand at terminals is the use of an inland port, which will act as an intermediate storage area before the cargoes are processed for export/import. Such an inland port could be made very efficient by automating all the tasks associated with processing, scheduling, storage, and transfer of containers between the inland port and the container terminals. An important part of such an automated system is the transport of containers using automated trucks. The use of automated trucks in cargo transportation will have the following benefits [2]:

- Automated and consistent container handling operation
- High container throughput
- Continuous operation: 24 hours a day, 365 days a year
- Reduced operational costs, especially labor costs
- High controllability and reliability
- High safety standards

In recent years, several studies have been carried out to investigate the feasibility of employing automated trucks for cargo transportation [2]. The Delta Terminal at Port of Rotterdam has been operating automated trucks referred to as Automated Guidance Vehicles (AGVs) for transporting containers within the terminal, while the Ports of Singapore, Thamesport, Hamburg, Kawasaki and Kaoshiung are experimenting with similar systems. In the Delta Terminal at Port of Rotterdam, a central controller instructs all AGVs where to go for new tasks. Each AGV weighs 14 tons, runs on a diesel hydraulic driveline and is capable of carrying up to 40-ton loads. The AGVs move along noiselessly at 6.8 mph, guided by transponders located beneath the pavement at 6.46 ft intervals. An overview picture is shown in Figure 1.

Deleted: -2

Figure 1. The Delta Port Container Terminal at Rotterdam.

Within the terminal, the travel distances are relatively short and the traffic is relatively high, therefore the automated trucks are operating at low speeds. The sensing, control and navigation problem becomes easier than at high speeds. However, if automated trucks are required to transport cargoes between a terminal and an inland port, generally a few miles away, they will be expected to travel at relatively higher speeds, which will make the vehicle control problem more challenging. The Center of Transport Technology in the Netherlands, studied a container transport system, called "Combi-Road" in 1994 [20]. Each container is pulled on a semi-trailer by an automated truck, as shown on the left side of Figure 2. The trucks are electrically driven and ride along specially designed tracks. The plan is to build a large system that would offer congestion-free transport of containers for a maximum distance of 200 km and at a maximum speed of 50km/h. A prototype vehicle has been successfully tested at an approximately 200 meters long test track.

Figure 2. Combi-Road.

Recently, a lot of research work has been done in the area of truck automation, automated highway systems and intelligent transportation systems. For example DaimlerChrysler has developed automatic vehicle following control systems for heavy-duty vehicles such as the "electronic draw bar" system [6]. Others include the Eaton-VORAD Collision Avoidance System that allows a truck to perform automatic vehicle following while maintaining safe time headway in traffic flow [5]. Lateral controllers like the Rapidly Adapting Lateral Position Handler (RAPLH) are used to steer buses/trucks along winding roads and change lanes to pass slower vehicles [5]. Another system for detecting lane departures, developed by Odetics ITS of Anaheim, California has been announced as an option for the Mercedes-Benz Actros truck/tractor in Europe, and is about to be introduced as an option by Mercedes' North American counterpart, Freightliner [5]. Furthermore, THOMSON-SCF DETEXIS, a company formed by an alliance between THOMSON-SCF and DASSAULT Electronique, is currently engaged in developing onboard electronics for advanced automotive products such as adaptive cruise control [7].

In the US, a lot of research efforts are currently under way to study the deployment of automated trucks on highways, as platoons or as autonomous vehicles, operating in mixed traffic [1, 9, 10, 14-17, 21]. At the Partners for Advanced Transit and Highways (PATH) there have been several research efforts on truck automation. A number of different longitudinal controllers, proposed and tested in [9, 14] with either linear or nonlinear spacing policies, allow automatic vehicle following in the longitudinal direction. It has been shown that the control strategies satisfy individual stability and string stability for a platoon of trucks. In the case of lateral control of heavy-duty trucks, classical loop-shaping, H-infinity loop-shaping and sliding mode control methods are tested and verified by experiments in [3]. Despite the past and recent activities in the area of truck automation, there is currently no system that utilizes fully automated trucks at

relatively high speeds. The development of longitudinal and lateral control laws that are robust and take advantage of existing sensor and communication technologies is still in its infancy.

In this project, we study an *Automated Cargo Transportation system between Inland POrt and Terminals* (ACTIPOT), which employs fully automated trucks to transfer cargoes between an inland port and the terminals. Since our approach focuses on the deployment of automated trucks in a controlled environment where human safety is not an issue, it could lead to the first implementation of fully automated trucks at high speeds. In our approach there will be a high variation in the loads carried by the automated trucks, i.e. containers could be empty or loaded and the truck could simply carry a chassis on its way to pick a container. The control laws should be such that they provide a reasonable response under all possible load variations, and are able to handle such variations without sacrificing performance and reliability. In our approach, trucks will not carry passengers or drivers. Issues such as driver comfort, and human factor concerns during transitions between automated and manual mode, that are present in systems such as adaptive cruise control and automated highway systems, will not be applicable. The use of automated trucks in the proposed ACTIPOT system are free of the human factors and liability issues that make the deployment of automated vehicles a wishful thinking of the future. In the ACTIPOT system the automated trucks will operate in a controlled environment in the absence of humans. As a result truck automation is feasible and it will be acceptable in the ACTIPOT environment provided it is designed properly and its benefits can be established.

The Report is organized as follows: In section 2 we describe the ACTIPOT system. In section 3 we present the truck dynamics, develop suitable longitudinal and lateral controllers, and analyze the closed-loop dynamics of automated trucks and platoons. In section 4 we design the supervisory controller that synchronizes the truck movements in the overall system. Microscopic simulation results that demonstrate the performance of the ACTIPOT system are presented in section 5. In Section 6 we present the conclusions.

2 THE ACTIPOT SYSTEM

Figure 3 shows a visual block diagram of the ACTIPOT system. Automated trucks are transferring containers between the inland port and a container terminal. These trucks are self-driven on a dedicated road that could be several miles long. The truck road may be dedicated for the automated trucks all the time or for time intervals, and the rest of the time could be used by manually driven vehicles. An automated truck employed in the ACTIPOT system will be assigned tasks such as carrying a container from the inland port, joining a platoon, speeding up to a desired velocity and cruising while on the road, slowing down when entering the container terminal, positioning itself under a quay crane for unloading, then getting loaded with an imported container and driving back to the inland port, and vice versa. Sensors on the road in conjunction with on-board the truck sensors, provide the appropriate measurements that are used by the on-board longitudinal and lateral control system in order to keep the truck at the center of the lane, track desired speeds and stop for loading and unloading. The focus of this research is to develop the operating characteristics of these trucks given the application under consideration, define the appropriate sensor and actuator characteristics and design longitudinal and lateral control systems that will provide full-automated capability. Simulations are carried out to demonstrate that each individual truck, with the developed longitudinal and lateral controllers, has the capability of driving in an autonomous mode and/or properly following a preceding truck. An overall system controller, which dictates and synchronizes the movements of the cranes and trucks in order to complete the work tasks in an efficient and safe manner, is designed and analyzed. In this project, a hypothetical ACTIPOT system is considered in the Long Beach area between the Intermodal Container Transfer Facility (ICTF) as an inland port and Pier G as a container terminal (see Figure 4 and 5). This information is used to select the routes and road structure for the dedicated lanes of the ACTIPOT system as shown in Figure 4.

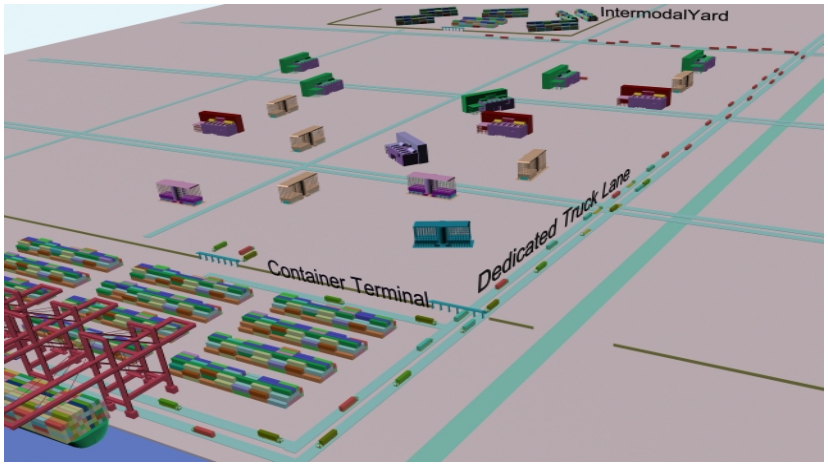

Figure 3. Automated trucks on dedicated lanes between an inland port and a container terminal.

Figure 4. Routine between ICTF ① and Port of Long Beach ②.

The Intermodal Container Transfer Facility (ICTF) (inland port), is denoted by ① in Figure 4, and Pier G (container terminal), is denoted by ②. The ICTF is operated by the Southern Pacific Railroad and is located approximately four miles away from the port of Long Beach. The dedicated lanes between ICTF and Pier G can be obtained by imbedding appropriate sensors on the existing roads and separating the automated traffic from the manual. In Figure 4, the purple line between ① and ② represents a feasible route for the ACTIPOT system. From ICTF to Pier G, the automated trucks can follow W. Willow Str., I-710, S. Harbor Scenic Dr., S. Pico Ave., and Pier G Ave., for a total route length of about 4.4 miles. The existing roads may need a few modifications to keep the road curvature small, so that automated trucks can travel at a relatively high speed, for a faster transfer of the containers. Apart from the road structure and distances no other data are used from the ICTF and Pier G terminal for the ACTIPOT system.

2.1 Design Considerations

The largest ships today are 17 containers wide and capable of carrying over 8,000 TEUs. A current service window expectation for mega-ships (over 6,000 TEUs) is 48 hours [2]. In the design of the ACTIPOT system, we consider the following conditions:

1. The Container Terminal (CT) is able to serve ships with capacity of 8,000 TEUs. It is assumed that the ships will arrive every 24 hours, which means the service time should be strictly limited to 24 hours or less. In our design, we further assume that the ship carries import containers up to 85% of its capacity and should be reloaded with the same number of export containers. The turnaround time for a ship with 85% load is

restricted to 20 hours, so that the system is able to serve any ship within 24 hours even if the ship is fully loaded and some unexpected events take place.

2. All the import containers will be transported to the inland port before they are distributed to different destinations, and all the export cargoes will be stored in the inland port before they are transferred to the CT. All the containers in the ACTIPOT system are of Forty-foot Equivalent Units (FEUs) type.

3. The maximum physical capacity of a quay crane is assumed to be 50 moves per hour in the single mode operation (i.e. either loading or unloading), and 42 moves per hour in the double mode (i.e. both loading and unloading). A variance of 15% to the maximum capacity of the quay cranes is considered, due to the uncertainties involved in the quay crane operations (i.e. variance in speed due to reaching different bays in the ship).

4. The maximum physical capacity of a crane in the inland port is assumed to be 60 moves per hour in the single mode. A variance of 15% is considered for this maximum capacity.

5. The automated trucks are able to work 24 hours per day. No fueling or maintenance time is considered for the trucks in this study.

2.2 ACTIPOT System Characteristics

The number of quay cranes, N_{qc}, required to accomplish the proposed task can be calculated by

$$N_{qc} = \left\lceil \frac{N_{container}}{C_{qc} T_{ship}} \right\rceil \tag{2-1}$$

where $N_{container}$ is the number of containers to be loaded/unloaded, C_{qc} is the maximum physical capacity of the quay cranes, T_{ship} is the desired ship turnaround time, and $\lceil \bullet \rceil$ is the operator that rounds up the argument to the closest integer. Using the specifications of section 2.1, we calculate that five quay cranes are required in order to load and unload a mega-ship with 3,400 containers of FEU within twenty hours.

As shown in Figure 5, the layout of the ACTIPOT system consists of three parts: The container terminal, the inland port and the dedicated lanes connecting the inland port with the terminal.

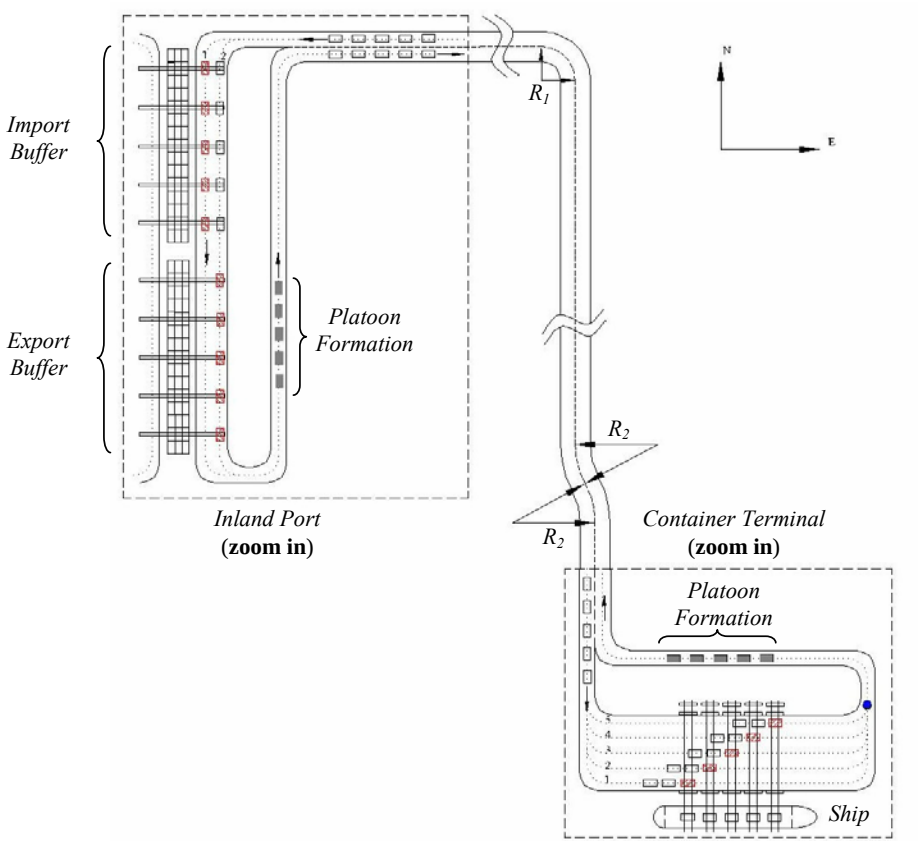

Figure 5. The layout for the ACTIPOT System.

The container terminal (Pier G), shown on the right lower box, is the place where ships are to be loaded or unloaded. The road curvature in this area may cause large transient lateral errors that may lead to a collision between two trucks traveling in opposite directions. Therefore all paths inside the container terminal are designed to be uni-directional so that large transient lateral errors will not cause serious problems. In this layout, five quay cranes are shown to serve the ship simultaneously. Each of the quay cranes can be accessed via the five service lanes under them. The service lane closest to the ship is labeled as 1, the second closest is labeled as 2 and so on. To simplify the control system logic without reducing the system efficiency, we assign Quay Crane 1 (QC1), which is the first crane from left side, to serve the trucks on service lane 1, QC2 to serve the trucks on service lane 2, and so on. At point P_1 the five service lanes merge together. To avoid collisions at this point, a time-window T_{w1} is established for P_1. When the system detects that one truck will reach P_1 at time t_1 while another truck will arrive at time t_2 and $|t_1 - t_2| < T_{w1}$, it will allow the truck closer to P_1 to pass first, while the other truck would wait until the collision possibility is eliminated. Platoon Formation

(PF) is the location where automated trucks are organized to form platoons. Assume that the PF is empty initially. When the first truck enters the PF it stays in pool 1. The second one enters and stays in pool 2, and so on until enough trucks have joined the platoon. For the proposed ACTIPOT system, we consider platoons of five trucks.

The inland port is shown in the left upper box of Figure 5. It has two buffers for import and export respectively and each buffer contains five cranes working in the single mode. Either of the two service lanes (labeled as 1 and 2) can access all the cranes. One platoon follows service lane 1 if available, otherwise it follows service lane 2. Similar to the container terminal, all the paths inside the inland port are uni-directional and a time-window T_{w2} is also established for the merging point P_2. There also exists a PF at the inland port to organize the trucks in platoons.

The dedicated lanes between the inland port and the container terminal are designed to be bi-directional, and automated trucks travel in platoon formations at relatively high speeds. In addition to being embedded with appropriate sensors, the existing paths should also be modified to eliminate large road curvatures. In Figure 5, some road curvatures are known and this knowledge is used in the design of the lateral controllers of the trucks, while the small unknown curvatures are treated as disturbances by the control system. For example, R_1=200m is known so that the curvature 1/200m^{-1} is taken into account by the lateral controller, and the road curvature associated with R_2=1,200m is treated as unknown disturbance.

3 AUTOMATED TRUCKS

An automated truck is a truck with an automatic control system that plays the role of a driver. It has the capability of full automation, such as tracking desired speed trajectories, following the preceding truck, tracing an assigned path, bypassing obstacles ahead, and so on. In this section, we investigate the dynamics of trucks that could be used for the ACTIPOT system, and design longitudinal and lateral controllers for truck automation.

3.1 Trucks for Container Transport

Figure 6 shows a Heavy-Duty Vehicle (HDV) used for experiments at PATH, which belongs to the class of those that can be used with the ACTIPOT system. It is a tractor semi-trailer vehicle with turbocharged diesel engine and automatic transmission. There is a so-called "fifth wheel", which links the tractor and the semi-trailer. In this project we took into account the modeling and control research work conducted under PATH for automated trucks.

Figure 6. The experiment HDV in PATH.

3.2 Truck Dynamics

Since an automated truck is expected to track the desired speed profile and follow the assigned path, the most essential outputs are the longitudinal position and velocity, and the lateral errors at the tractor front axis, the tractor rear axis and the trailer rear axis. The inputs to be generated by the onboard controllers are the fuel, brake and steering commands. As with human driving, we assume that the fuel and brake commands are not issued at the same time. Strictly speaking, the longitudinal and lateral dynamics of a truck are coupled together, which means the longitudinal velocity and lateral errors are both affected by the fuel/brake and steering commands simultaneously. Due to this coupling, the full order dynamics of a HDV are very complicated and difficult to analyze.

However, under some reasonable assumptions, we can decouple the truck model to a longitudinal model and a lateral model. These assumptions are

- The truck varies its velocity only when the road is straight (or the road curvature is very small).
- The truck maintains a constant speed (or close to a constant speed) when the road curvature is large.

By designing the control system so that these two assumptions are valid, the truck's longitudinal velocity can be controlled by the fuel/brake command while the truck's lateral errors are only affected by the steering command.

3.2.1 Longitudinal Dynamics

A nonlinear longitudinal truck model [9, 13] involving the diesel engine, automatic transmission and drivetrain is presented in Appendix B. The input to this model is fuel/brake command, and the output is the longitudinal acceleration. This model contains six states and is detailed enough to capture all the important longitudinal dynamics of a tractor semi-trailer vehicle. Among the six states of the longitudinal model, the dominant state is the one associated with the truck longitudinal velocity v, which is determined by

$$\dot{v} = \frac{F_t - F_a - F_r}{m} \tag{3-1}$$

where m is the vehicle mass, F_t is the tractive tire force, F_a is the aerodynamic drag force, and F_r is the rolling friction force. In (3-1),

$$\begin{cases} F_a = c_a v^2 \\ F_r = \dfrac{c_r mg}{h_w} \end{cases} \tag{3-2}$$

where c_a is the aerodynamic drag coefficient, c_r is the rolling friction coefficient, h_w is the radius of the front wheels, g is the gravity constant, and the brake/fuel commands are incorporated in the differential and algebraic equations that determine the tractive tire force F_t. In our analysis and simulations, the situation that both fuel and brake commands are issued at the same time does not exist. Therefore, the turbine torque M_T is considered to be zero if a brake command appears, while the brake torque M_b is zero if there is a nonzero fuel command. More details about the model are given in Appendices A and B.

3.2.2 Lateral Dynamics

For the lateral control of a tractor semi-trailer vehicle, we are only interested in the lateral and yaw motions. A simplified lateral model [18] with respect to the road reference frame presented in detail in Appendix C, has the form

$$\overline{M}\ddot{q}_r + D\dot{q}_r + \overline{K}q_r = F\theta_w + E_1\dot{\varepsilon}_d + E_2\ddot{\varepsilon}_d \tag{3-3}$$

where $q_r = \begin{bmatrix} y_r & \varepsilon_r & \varepsilon_f \end{bmatrix}^T$, y_r is the lateral displacement of tractor's center of gravity (CG) with respect to the road center line, ε_r is the yaw angle of the tractor relative to the road center line, and ε_f is the relative yaw angle between the tractor and the semi-trailer. The input to this model is the front wheel angle θ_w, and $\dot{\varepsilon}_d$ and $\ddot{\varepsilon}_d$ are road curvature characteristics and can be considered as disturbances when small and taken into account when large.

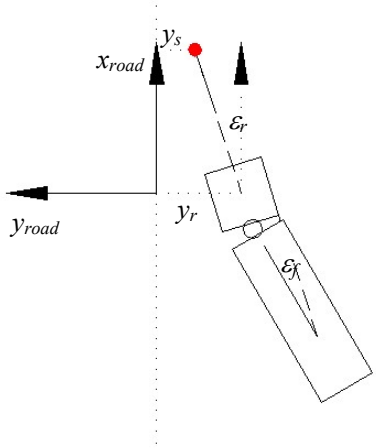

Figure 7. A truck in the road reference frame.

A complete lateral model also includes the steering angle, which is not shown in (3-3). The steering system is composed of steering wheel and column, the power assistance unit, the steering linkages connecting the hydraulic power steering unit to the front wheel assembly, and some other parts. The turning of the steering wheel by angle θ_s results in a vehicle turning wheel angle θ_w, which is the input variable in (3-3). In [3], it has been shown that if a good inner loop controller is used, the closed-loop steering system can be approximated as a first order system. In our control design and simulations, this closed-loop steering system is approximated by $G_A(s)$, which has the form

$$G_A(s) = \frac{\theta_w(s)}{\theta_s(s)} = \frac{1}{0.08s + 1} \tag{3-4}$$

Therefore, the complete lateral model is described by (3-3) and (3-4).

3.3 Control Design for Truck Automation

3.3.1 Longitudinal Control Design for Speed Tracking

In the speed tracking case, the longitudinal controller is designed so that the truck is able to track desired speed trajectories. The longitudinal model presented in Appendix B is sixth-order and highly nonlinear, thus not suitable for control design. Since the mode associated with the truck velocity is always much slower than those associated with the other five states, the longitudinal truck model can be viewed as a first-order nonlinear system:

$$\dot{v} = f(v,u) \tag{3-5}$$

where v is the truck velocity and u is the fuel/brake command. This nonlinear model can be linearized around operating points corresponding to steady state, i.e.

$$\dot{v} = -a(v - v_d) + b(u - u_d) + d \tag{3-6}$$

where v_d is the desired steady state velocity, u_d is the corresponding steady state fuel command, d is the modeling uncertainty, and a and b are positive parameters that depend on the operating point, i.e. on the steady state values of the vehicle speed and load torque. For a given vehicle, the relation between v_d and u_d is described by a look-up table, or a 1-1 mapping continuous function

$$v_d = f_u(u_d) \tag{3-7}$$

Theorem 3.1: For a system represented in (3-6, 3-7), the control law

$$u = f_u^{-1}(v_d) + k_p(v_d - v) + k_i\int_0^t (v_d - v)d\tau + k_d\frac{d}{dt}(v_d - v) \tag{3-8}$$

where k_p, k_i, k_d are some positive parameters, can stabilize the closed-loop system. In addition, if v_d and d are constants, then $(v_d - v) \to 0$ as $t \to \infty$.

Proof: Substituting (3-8) into (3-6) and taking the Laplace transform, we obtain

$$v(s) = \frac{\Delta(s) - s^2}{\Delta(s)}v_d(s) + \frac{s[-bk_d v_d(0) + (1 + bk_d)v(0)]}{\Delta(s)} + \frac{sd(s)}{\Delta(s)} \tag{3-9}$$

where $\Delta(s)=(1+bk_d)s^2+(a+bk_p)s+bk_i$, and $v_d(0)$ and $v(0)$ are the initial values for v_d and v. It follows that

$$(v_d-v)(s)=\frac{s^2}{\Delta(s)}v_d(s)+\frac{s[bk_dv_d(0)-(1+bk_d)v(0)]}{\Delta(s)}-\frac{sd(s)}{\Delta(s)} \tag{3-10}$$

Recall that *a* and *b* are positive and k_p, k_i, k_d are also chosen positive, thus $\Delta(s)$=0 has stable roots. If v_d and d are constants, then $d(s)=d\frac{1}{s}$ and $v_d(s)=v_d\frac{1}{s}$, and then

$$\lim_{t\to\infty}(v_d-v)(t)=\lim_{s\to 0}s\left[\frac{s}{\Delta(s)}v_d+\frac{s[bk_dv_d(0)-(1+bk_d)v(0)]}{\Delta(s)}-\frac{1}{\Delta(s)}d\right]=0 \tag{3-11}$$

Remark: From $\Delta(s)=(1+bk_d)s^2+(a+bk_p)s+bk_i$, we can see that k_p should be chosen large enough for faster convergence of (v_d-v) to zero. If d is not a constant but varies slowly with time, which means $\lim_{s\to 0}\left(\frac{s^2d(s)}{\Delta(s)}\right)\approx 0$, then it will have little impact on the steady state velocity error.

In practice, the desired speed trajectory cannot vary fast due to the inherent low actuation-to-weight ratio of HDVs, thus the desired fuel command trajectory $f_u^{-1}(v_d)$ does not vary fast, either. In this case, $f_u^{-1}(v_d)$ can be viewed as a part of d and removed from the control law with almost no impact on performance as at steady state, the integral action in (3-8) can compensate for the absence of $f_u^{-1}(v_d)$. In (3-8) the acceleration signal is made available by differentiating the velocity data, so that the acceleration measurement is not necessary. In our application, an approximated differential term is used to avoid the "dirty jerk" in the velocity measurement. Hence the revised control law becomes

$$u=k_pe_v+k_i\frac{1}{s}e_v+k_d\frac{s}{\frac{1}{N}s+1}e_v \tag{3-12}$$

where N is a sufficiently large positive number. According to (3-12), a fuel command is issued when u is positive, while the brake is activated when u is negative. The control output is multiplied by a fixed gain when it is negative because of the different actuator limits. A hysteresis element is placed after the controller to avoid chattering between fuel and brake. This element can be viewed as a simplified switching rule that decides when to use the fuel or brake controller [9].

The Matlab Simulink software (by MathWorks) is used to simulate the proposed control law in (3-12). In the simulations, the full nonlinear model presented in Appendix B is used and the three parameters in the control law are chosen as $k_p=150$, $k_i=3$ and

$k_d = 20$. As shown in Figure 8, the dashed line is the desired speed trajectory and the solid line is the truck's speed response. Initially, the speed command is 12m/sec. After 20 seconds, the desired speed goes up by 0.2m/sec^2 for 20 seconds, stays at 16m/sec for another 20 seconds, drops down by -2m/sec^2 for 4 seconds, and then stays at 8m/sec. From the speed error response shown in Figure 9, it can be seen that the absolute speed error is less than 0.25m/sec during the acceleration and 1.5m/sec during the deceleration. Further simulations performed using 50% uncertainty in the mass have shown similar responses, which indicates that the proposed control law in (3-12) is robust enough for our application.

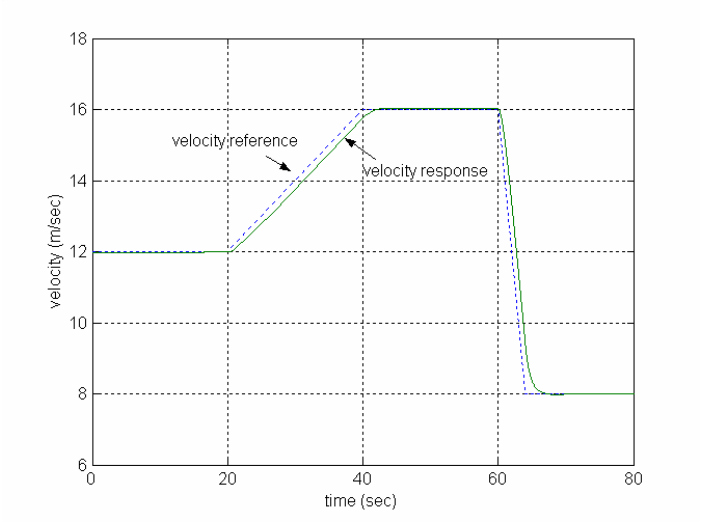

Figure 8. Speed response of the HDV.

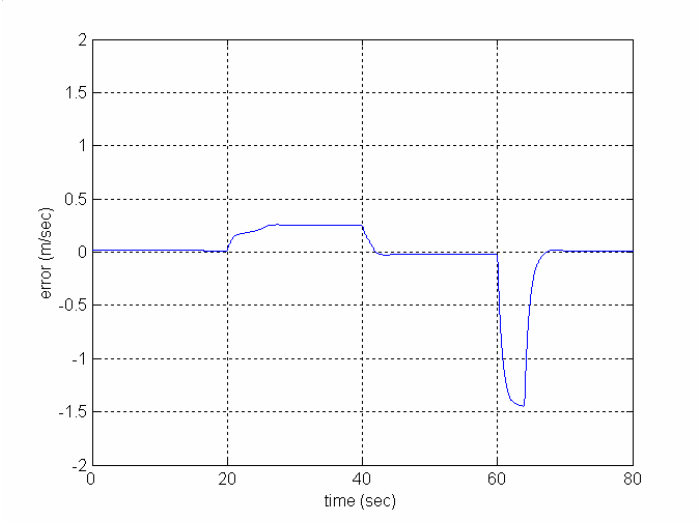

Figure 9. The speed error during the speed tracking.

3.3.2 Longitudinal Control Design for Vehicle Following

In Automated Highway Systems (AHS), a widely accepted strategy for effectively increasing highway throughput is to group automatic vehicles in tightly spaced formation called *platoon*. An individual vehicle (except the leading one) within the platoon should be able to follow the preceding one tightly, and collision-free operation should be guaranteed for all possible maneuvers. In the ACTIPOT system, utilization of platoons to improve traffic throughput indicates that cargoes can be transported faster and the system efficiency can be improved. Utilization of platoons can also reduce the system complexity since collision-free operation is guaranteed within a platoon without involving the central computer. Furthermore, in a controlled environment, since the intervehicle spacing in a platoon are reduced, the average spacing between two platoons can be increased. This will help improve the system safety and reduce unnecessary decelerations and stops.

The control design for truck following has to guarantee not only a desired performance for individual trucks but also stability for the whole platoon referred to as *string stability* [1, 12]. String stability in a platoon implies that any nonzero separation, velocity and acceleration error of an individual truck in a string of trucks does not get amplified as it propagates upstream [1, 12].

A platoon composed of M trucks can be modeled as

$$v_i = G_i(s)v_{i-1} \tag{3-13}$$

where $2 \le i \le M$, v_i is the velocity of the *i*th truck and $G_i(s)$ is a proper stable transfer function that represents the input-output behavior of the *i*th truck. The velocity error v_r, acceleration error a_r and separation error δ for the *i*th truck are defined as

$$\begin{cases} v_{ri} = v_{i-1} - v_i \\ a_{ri} = a_{i-1} - a_i \\ \delta_i = x_{ri} - s_{di} \end{cases} \tag{3-14}$$

where x_{ri} is the separation distance between the *i*-1th and the *i*th trucks, and s_{di} is the desired separation distance between the *i*-1th and the *i*th trucks. A demonstration of one truck following another is shown in Figure 10.

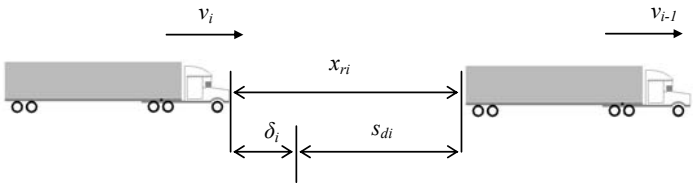

Figure 10. Diagram of the truck following mode.

Definition 3.1: A platoon is said to be *string stable* if [1]

$$\begin{cases} \|v_{ri}\|_p \le \|v_{ri-1}\|_p \\ \|a_{ri}\|_p \le \|a_{ri-1}\|_p, \\ \|\delta_i\|_p \le \|\delta_{i-1}\|_p \end{cases} \quad \forall p \in [1, +\infty], \forall i \text{ with } 2 \le i \le M \tag{3-15}$$

Definition 3.2: A platoon is said to be *L_2 string stable* if [9]

$$\begin{cases} \|v_{ri}\|_2 \le \|v_{ri-1}\|_2 \\ \|a_{ri}\|_2 \le \|a_{ri-1}\|_2, \\ \|\delta_i\|_2 \le \|\delta_{i-1}\|_2 \end{cases} \quad \forall i \text{ with } 2 \le i \le M \tag{3-16}$$

L_2 string stability is a particular case of (3-15), in which $p = 2$. It means the energy (represented by the L_2 norm) of the output error is not larger than the energy of the input error. In this report, we will deal with L_2 string stability. If the error transfer function in

a system like (3-13) is $G_e(s)$, L_2 string stability is equivalent to $\|G_e(j\omega)\|_\infty \le 1$ for all ω [9]. In [16] it was shown that string stability cannot be achieved with constant intervehicle spacing under autonomous operations. However string stability can be guaranteed if a time headway policy [21] is used for the intervehicle spacing and the controller gains are chosen appropriately. With the time headway policy the desired intervehicle spacing is given by

$$s_{di} = s_0 + hv_i \tag{3-17}$$

where s_0 is a fixed safety distance at low speeds and h is referred to as the time headway.

The vehicle following controller to be designed should guarantee that $v_{ri} \to 0$ and $\delta_i \to 0$ with time for each individual truck in the platoon, and also guarantee string stability for the whole platoon. We first evaluate the individual truck behavior and then analyze string stability for the whole platoon. In order to simplify notation, the subscript i is omitted, and the symbols v_l and v_f are used to denote v_{i-1} and v_i respectively. In our work, we consider the nonlinear spacing policy proposed in [14], which has been demonstrated to reduce the intervehicle spacing significantly.

Theorem 3.2: Suppose h and k are selected as

$$\begin{cases} h = sat(h_0 - c_h v_r) \\ k = c_k + (k_0 - c_k)e^{-\sigma\delta^2} \end{cases} \tag{3-18}$$

where h_0, c_h, k_0, c_k and σ are positive constants to be designed and $c_k < k_0$. The saturation function $sat(\bullet)$ has an upper bound 1 and lower bound 0. If v_l is a constant, then

$$v_r \to 0, \delta \to 0 \Leftrightarrow v_r + k\delta \to 0 \tag{3-19}$$

for some h_0, c_h, k_0, c_k and σ.

Proof: It is trivial to see that $v_r \to 0, \delta \to 0 \Rightarrow v_r + k\delta \to 0$, provided k_0, c_k and σ are positive and finite. Thus we only need to establish the reverse, i.e., when the control objective $v_r + k\delta \equiv 0$ is achieved, both the relative velocity v_r and the separation error δ converge to zero [9]. It can be seen that

$$v_r + k\delta \equiv 0 \Rightarrow \dot{v}_r + \dot{k}\delta + k\dot{\delta} \equiv 0 \tag{3-20}$$

From $v_r = v_l - v_f$ and v_l is a constant, we know

$$\dot{v}_r = -\dot{v}_f \tag{3-21}$$

By differentiating both sides of $\delta = x_r - (s_0 + hv_f)$, we obtain

$$\dot{\delta} = v_r - h\dot{v}_f - \dot{h}v_f = -k\delta - (h + \alpha(h)c_h v_f)(\dot{k}\delta + k\dot{\delta}) \tag{3-22}$$

where

$$\alpha(h) = \begin{cases} 1, & 0 < h < 1 \\ 0, & \text{otherwise} \end{cases} \tag{3-23}$$

With k in (3-17), (3-21) becomes

$$\left\{1 + (h + \alpha(h)c_h v_f)\left[c_k + (1 - 2\sigma\delta^2)(k_0 - c_k)e^{-\sigma\delta^2}\right]\right\}\dot{\delta} + k\delta = 0 \tag{3-24}$$

In (3-24), $c_k + (1 - 2\sigma\delta^2)(k_0 - c_k)e^{-\sigma\delta^2}$ achieves its minimum $c_k - 2(k_0 - c_k)e^{-3/2}$ at $\delta = \pm\sqrt{3/2\sigma}$. If $c_k - 2(k_0 - c_k)e^{-3/2} \geq 0$, the coefficient of $\dot{\delta}$ is always larger than 1. Thus $\delta \to 0$ as $t \to \infty$. If $c_k - 2(k_0 - c_k)e^{-3/2} < 0$ and h_0 and c_h are chosen so that

$$0 < h < \frac{-1}{c_k - 2(k_0 - c_k)e^{-3/2}} \tag{3-25}$$

then the coefficient of $\dot{\delta}$ is always positive. Therefore $\delta \to 0$ as $t \to \infty$. From $v_r + k\delta \equiv 0$, we can see that $\delta \to 0$ as $t \to \infty$ implies $v_r \to 0$ as $t \to \infty$.

Remark: In the proof, we have used $\dot{h} = \alpha(h)c_h\dot{v}_r$. Strictly speaking this is not true because h is not differentiable with respect to v_r when $v_r = h_0/c_h$, or $(h_0 - 1)/c_h$. However, $\forall \varepsilon > 0$, there always exists a differentiable function $\tilde{h}(v_r)$, which differs from h on the set $\Omega = \{v_r \mid h_0/c_h - \varepsilon < v_r < h_0/c_h + \varepsilon, \text{or } (h_0 - 1)/c_h - \varepsilon < v_r < (h_0 - 1)/c_h + \varepsilon\}$, and $-c_h \leq \frac{d\tilde{h}}{dv_r} \leq 0$ on Ω. Such a differentiable function $\tilde{h}(v_r)$ will make the proof more rigorous, and the h in (3-18) can be viewed as a practical approximation of $\tilde{h}(v_r)$.

From the above theorem, it follows that the regulation of $v_r + k\delta$ to zero implies that the relative velocity and separation error are also regulated to zero. Therefore, the control objective in the vehicle following mode is $v_r + k\delta \to 0$. The longitudinal model in (3-5) is linearized along the leading car's speed trajectory v_l and the corresponding steady state input. The simplified linear model is

$$\dot{v}_f = -a(v_f - v_l) + b(u - u_d) + d \tag{3-26}$$

where $u_d = f_u^{-1}(v_l)$. If we denote the control objective $v_r + k\delta$ by J and linearize it at the steady states where $v_r = 0$ and $\delta = 0$, we have

$$J = v_r + k_0\delta + R_1 \tag{3-27}$$

where R_1 is the remainder term due to linearization. Further assume that the variation of v_r is small enough to keep h away from saturation and v_l varies slightly around its nominal value v_{l0}, then

$$\delta = x_r - s_0 - (h_0 + c_h v_{l0})v_f + c_h v_{l0} v_l + R_2 \tag{3-28}$$

where R_2 is the remainder term. From equations (3-27) and (3-28), we obtain

$$J = -k_1 v_f + k_2 v_l + k_0 x_r - k_0 s_0 + d^* \tag{3-29}$$

where $k_1 = 1 + k_0 h_0 + c_h k_0 v_{l0}$, $k_2 = 1 + c_h k_0 v_{l0}$ and $d^* = R_1 + k_0 R_2$. If $\dot{d}^*$ is small enough, by differentiating (3-29) and neglecting $\dot{d}^*$, we obtain

$$\dot{J} = -k_1 \dot{v}_f - k_0 v_f + k_2 \dot{v}_l + k_0 v_l \tag{3-30}$$

The control objective now is equivalent to minimizing J specified by (3-29).

Remark: If we set c_h and σ to zero and neglect the high order term d^*, then (3-29) becomes $J = v_r + k_0(x_r - s_0 - h_0 v_f)$, and at the same time (3-18) gives $h = h_0$ and $k = k_0$. This implies the spacing policy involving constant h and k is a special case of the linearized spacing policy with variable h and k in (3-18).

Theorem 3.3: For a linear system represented by (3-26, 3-29), if $v_l \equiv v_{l0}$ and d^* and its derivative are negligible, then for some positive k_p, k_i, k_d the control law

$$u = f_u^{-1}(v_d) + k_p J + k_i \int_0^t J d\tau + k_d \frac{dJ}{dt} \tag{3-31}$$

leads to a stable closed-loop system. If d in (3-24) is a constant, then $J \to 0$ as $t \to \infty$.

Proof: Given $v_l \equiv v_{l0}$, (3-30) can be transformed to

$$J(s) = -\frac{k_1 s + k_0}{s} v_f(s) + \frac{k_0}{s^2} v_{l0} + \frac{J(0) + k_1 v_f(0)}{s} \tag{3-32}$$

and (3-26) can be transformed to

$$v_f(s) = \frac{a}{s(s+a)} v_{l0} + \frac{b}{s+a}(u(s) - u_d(s)) + \frac{1}{s+a} d(s) + \frac{v_f(0)}{s+a} \tag{3-33}$$

Using (3-31), we get

$$J(s) = \frac{(k_0 - ak_1)s}{\Gamma(s)} v_{l0} - \frac{(k_1 s + k_0)s}{\Gamma(s)} d(s) + \frac{[(bk_1 k_d + 1)s + (bk_0 k_d + a)]s}{\Gamma(s)} J(0) + \frac{(ak_1 - k_0)s}{\Gamma(s)} v_f(0) \tag{3-34}$$

where $\Gamma(s) = (1 + bk_1 k_d)s^3 + (a + bk_0 k_d + bk_1 k_p)s^2 + (bk_1 k_i + bk_0 k_p)s + bk_0 k_i$. Since k_p, k_i, k_d are positive constants, the four coefficients in $\Gamma(s)$ are all positive. From Routh's stability criterion, $\Gamma(s)$ is stable if and only if

$$(a + bk_0 k_d + bk_1 k_p)(bk_1 k_i + bk_0 k_p) > bk_0 k_i (1 + bk_1 k_d) \tag{3-35}$$

or equivalently

$$(a + bk_1 k_p)(k_1 k_i + k_0 k_p) + bk_0^2 k_p k_d - k_0 k_i > 0 \tag{3-36}$$

Obviously, there always exist constants k_p, k_i, k_d to satisfy (3-36). For example, if we fix k_i, then sufficiently large k_p and k_d will satisfy (3-34). If d is a constant, then $d(s) = d\frac{1}{s}$, and then

$$\lim_{t \to \infty} J(t) = \lim_{s \to 0} sJ(s) = 0 \tag{3-37}$$

Remark: The closed-loop system is stable if and only if k_p, k_i, k_d are chosen so that (3-34) holds. One sufficient condition for the system stability is $k_p > k_i / a$ for all possible values of a. However, smaller k_i leads to a root of $\Gamma(s) = 0$ closer to zero, which puts the constraint that k_i should be kept away from zero.

For the linear system described by (3-26, 3-29, 3-31), if the leading truck's velocity varies slowly around v_{l0}, then

$$\frac{v_f}{v_l} = G_v(s) = \frac{bk_2 k_d s^3 + (a + bk_0 k_d + bk_2 k_p)s^2 + (bk_2 k_i + bk_0 k_p)s + bk_0 k_i}{\Gamma(s)} \tag{3-38}$$

The values of a and b in (3-26) depend on the nominal velocity v_{l0}. If all the trucks in the platoon have identical input-output characteristics and the separation errors are small enough to be approximated by (3-28), then it is trivial to see that

$$\frac{v_{ri}}{v_{ri-1}} = \frac{a_{ri}}{a_{ri-1}} = \frac{\delta_i}{\delta_{i-1}} = \frac{v_i}{v_{i-1}} = G_v(s) \tag{3-39}$$

Theorem 3.4: The linear system represented by (3-26, 3-29, 3-31) can be made L_2 string stable if the three controller parameters k_p, k_i, k_d are properly chosen.

Proof: Rewrite the transfer function in (3-38) as

$$G_v(s) = \frac{a_3 s^3 + a_2 s^2 + a_1 s + a_0}{b_3 s^3 + b_2 s^2 + b_1 s + b_0} \tag{3-40}$$

where $a_i > 0$ and $b_i > 0$ for i=0, 1, 2 and 3. The linear system (3-26, 3-29, 3-31) is L_2 string stable if and only if $\|G_v(j\omega)\|_\infty \le 1$, and

$$\|G_v(j\omega)\|_\infty \le 1 \Leftrightarrow \frac{\left(-a_3\omega^3 + a_1\omega\right)^2 + \left(-a_2\omega^2 + a_0\right)^2}{\left(-b_3\omega^3 + b_1\omega\right)^2 + \left(-b_2\omega^2 + b_0\right)^2} \le 1, \forall\, \omega \in [0, +\infty) \tag{3-41}$$

After manipulating the right inequality in (3-41) and using the fact that $a_0 = b_0 = bk_0k_i$, we get $\|G_v(j\omega)\|_\infty \le 1$ is equivalent to: $\forall\, \omega \in [0, +\infty)$,

$$\left(b_3^{\,2} - a_3^{\,2}\right)\omega^4 + \left(b_2^{\,2} - a_2^{\,2} - 2b_1b_3 + 2a_1a_3\right)\omega^2 + \left(b_1^{\,2} - a_1^{\,2} - 2b_0b_2 + 2a_0a_2\right) \ge 0 \tag{3-42}$$

It can be seen that

$$b_3^{\,2} - a_3^{\,2} = \left(1 + bk_1k_d\right)^2 - \left(bk_2k_d\right)^2 > 0 \tag{3-43}$$

and

$$b_1^{\,2} - a_1^{\,2} - 2b_0b_2 + 2a_0a_2 = b^2h_0k_0k_i^{\,2}\left(k_1 + k_2\right) > 0 \tag{3-44}$$

Therefore, $\|G_v(j\omega)\|_\infty \le 1$ is equivalent to

$$\begin{aligned} &b_2^{\,2} - a_2^{\,2} - 2b_1b_3 + 2a_1a_3 \ge 0, \text{ or} \\ &\left(b_2^{\,2} - a_2^{\,2} - 2b_1b_3 + 2a_1a_3\right)^2 - 4\left(b_3^{\,2} - a_3^{\,2}\right)\left(b_1^{\,2} - a_1^{\,2} - 2b_0b_2 + 2a_0a_2\right) \le 0 \end{aligned} \tag{3-45}$$

A sufficient condition for satisfying (3-43) would be $b_2^{\,2} - a_2^{\,2} - 2b_1b_3 + 2a_1a_3 \ge 0$, which implies

$$b^2\left(k_1^{\,2}-k_2^{\,2}\right)k_p^{\,2}+2\left(a+bk_0k_d-bh_0k_0^{\,2}k_d-bk_0\right)k_p-2bk_1k_i-2b^2k_dk_i\left(k_1^{\,2}-k_2^{\,2}\right)\geq 0 \tag{3-46}$$

If we choose $k_d > \dfrac{1}{1-h_0k_0}$ and $k_p > \sqrt{\dfrac{2k_1k_i}{bh_0k_0\left(k_1+k_2\right)}+2k_dk_i}$, (3-46) will always hold, and therefore the linear system represented by (3-26, 3-29, 3-31) is L_2 string stable for some choices of the controller parameters.

In our application, the control law is chosen as

$$u=k_p\left(v_r+k\delta\right)+k_i\frac{1}{s}\left(v_r+k\delta\right)+k_d\frac{s}{\frac{1}{N}s+1}\left(v_r+k\delta\right) \tag{3-47}$$

Again the approximated derivative action term is employed in the control law to avoid any non-smooth measurements in $v_r+k\delta$, and the term $f_u^{-1}\left(v_l\right)$ has been removed. Theorems 3-3 and 3-4 are valid only for the linearized truck dynamics and spacing policy. The proposed control law must be further tested and verified via simulations, involving the nonlinear truck model and spacing policy.

We simulate a platoon of five identical trucks. The control parameters are chosen as $h_0=0.1$, $c_h=0.2$, $k_0=1$, $c_k=0.1$, $\sigma=0.1$, $k_p=150$, $k_i=3$ and $k_d=20$. The speed trajectory used in the speed tracking case is issued to the leading truck. Figure 11 shows the speed responses of the five HDVs in the platoon. In this figure, the thickest line is associated with $i=1$, the second thickest line is associated with $i=2$ and so on. The relative velocity v_{ri}, separation distance x_{ri} and separation error δ_i responses are shown in Figure 12, 13 and 14 respectively. In the platoon case, the separation distance between two trucks is most important since it implies collision when negative. From Figure 13, we see that the intervehicle spacing has been compressed to less than 5m, but it is always larger than 3m even during the deceleration period. A platoon composed of five trucks with different weights has also been simulated. Despite a 50% variation in the trailer mass, the simulation results are very similar to those obtained for the platoon of five identical trucks. Therefore our simulations demonstrate that the proposed longitudinal control law in (3-47) is robust with respect to the load mass, and it can provide desired platoon performance for the ACTIPOT system.

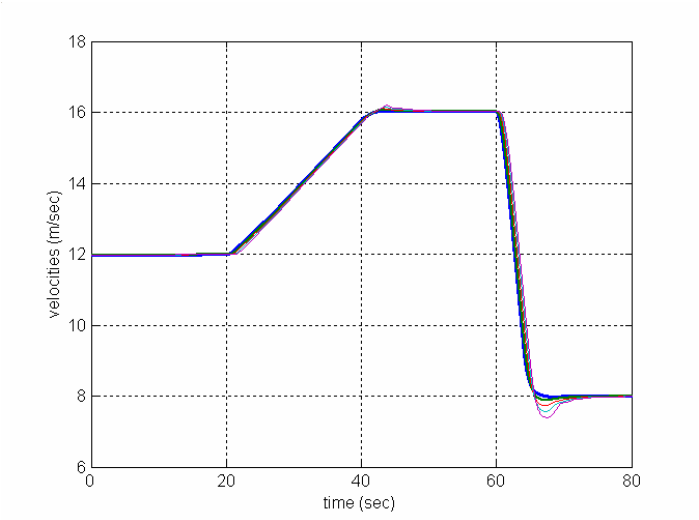

Figure 11. Velocities v_i of the five HDVs in the platoon.

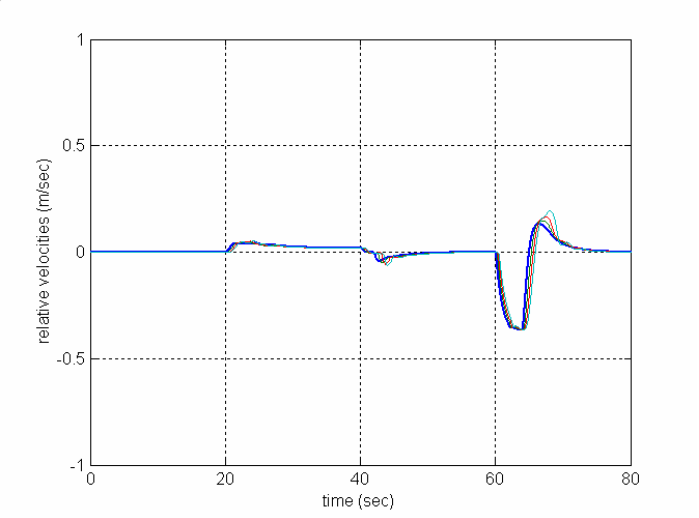

Figure 12. Relative velocities v_{ri}.

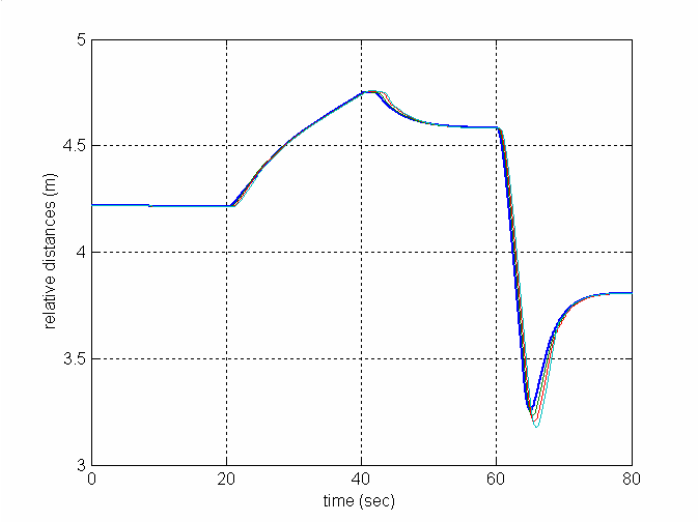

Figure 13. Separation distances x_{ri}.

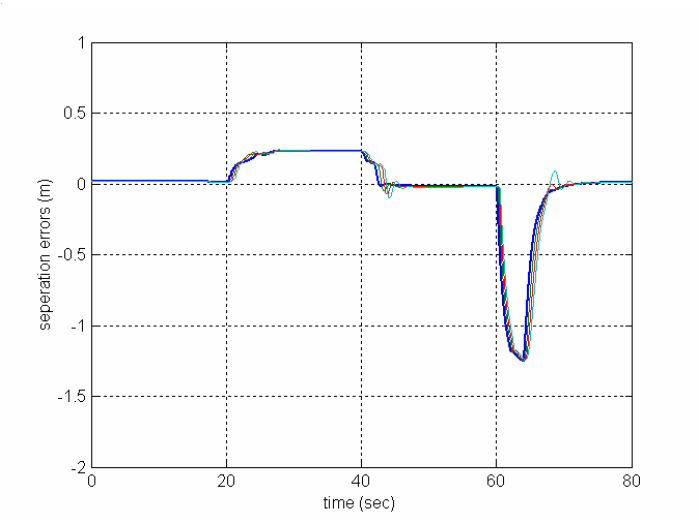

Figure 14. Separation errors δ_i.

3.3.3 Lateral Control Design

The transfer function from θ_s to y_r is obtained from (3-3) and (3-4). It contains a pair of poorly-damped zeros when the longitudinal velocity is high, which makes the lateral control difficult if the lateral error at the tractor's center of gravity (CG) is the only signal used for feedback. This problem can be solved by introducing a *look-ahead distance* d_s [3]. As shown in Figure 7, it is assumed that a virtual sensor is placed at distance d_s ahead of the tractor CG, and its measurement y_s is used for feedback. It is easy to see that

$$y_s = y_r + d_s \varepsilon_r \tag{3-48}$$

The transfer function from θ_s to y_s, $G_o(s)$, is obtained from (3-3), (3-4) and (3-48). Model uncertainties in $G_o(s)$ may be due to variations in trailer mass m_2, longitudinal velocity $\dot{x}_u$ and road adhesion coefficient μ. In this section, we design a robust lateral controller using the McFarlane and Glover loop-shaping method to deal with the model uncertainties.

The H-infinity robust stabilization combined with classical loop shaping method, proposed by McFarlane and Glover [22], consists of two design steps. First, the open-loop plant is augmented using pre- and post-compensators, W_1 and W_2 respectively, to achieve a desired shape for the singular values of the open-loop frequency response. The augmented plant is denoted as G_s. Secondly, a robust with respect to a coprime factor uncertainty controller, K_s, is developed to stabilize G_s using H-infinity optimization. An important advantage for this method is that no uncertainty weight is required in the second step. In the control design, d_s is selected to be 5m, and the nominal values for the variable parameters are m_2 =15,000kg, $\dot{x}_u$ =20.1m/sec and $\mu = 0.8$. The pre- and post-compensators are selected as

$$W_1 = 10 \tag{3-49}$$

and

$$W_2 = \frac{1}{5s+1} \tag{3-50}$$

The Bode plots of the developed H-infinity robust lateral controller are shown in Figure 15. Figures 16 and 17 show that the compensated system has good frequency response properties, and the gain margin and phase margin indicate that the closed-loop system has good stability properties.

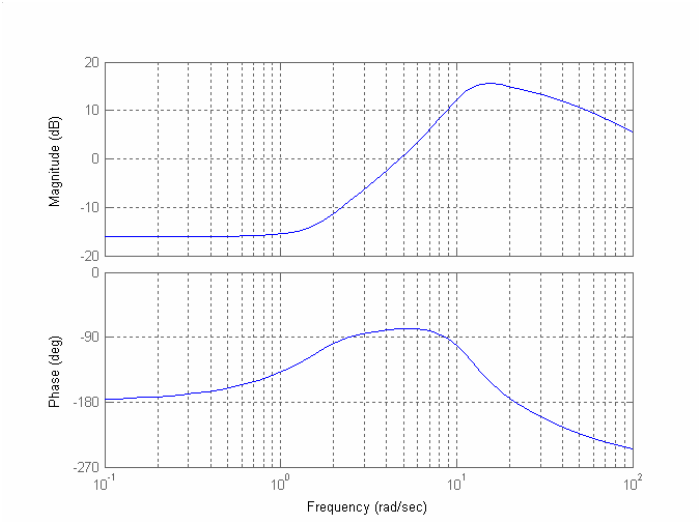

Figure 15. Bode plots of the H-infinity controller $K_s(s)$.

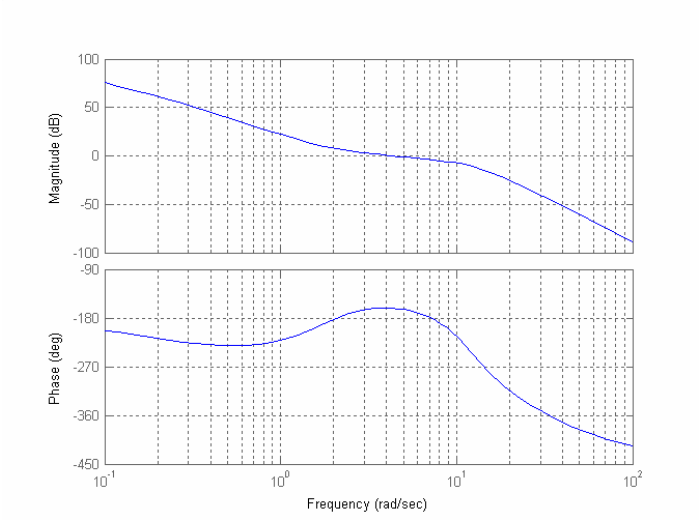

Figure 16. Bode plots of the compensated open-loop system $G_c(s)$.

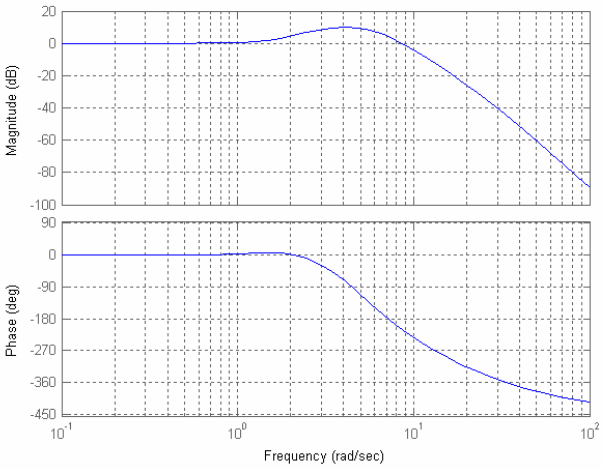

Figure 17. Bode plots of the closed-loop system $L_c(s)$.

In the simulation, the HDV is required to follow the path shown in Figure 18 with a constant speed of 45 miles/hour (about 20.1m/sec). It is desired that the body of the HDV should lie within the assigned lane, as shown in Figure 19. The average width of an HDV, from left mirror to the right one, is about 2.8m while US highway lanes have the width of 3.6m [8]. Therefore, the worst lateral error should be less than 0.4m. The parameters used in the simulation are at their nominal values. A time delay of 15ms is included into the steering system to make the steering model closer to the practical system. Since the road curvature is small ($\pm 1/800\text{m}^{-1}$), it is treated as a disturbance. The steering angle issued by the control system is shown in Figure 20, and the lateral errors are shown in Figure 21. From Figure 21 we can see that the proposed controller has good performance and the largest transient error is less than 0.1m. By varying m_2 between 5,000kg and 25,000kg, $\dot{x}_u$ between 3m/s and 28m/s, and μ between 0.5 and 1, the lateral errors are still less than 0.4m, which demonstrates the robustness properties of the proposed lateral controller.

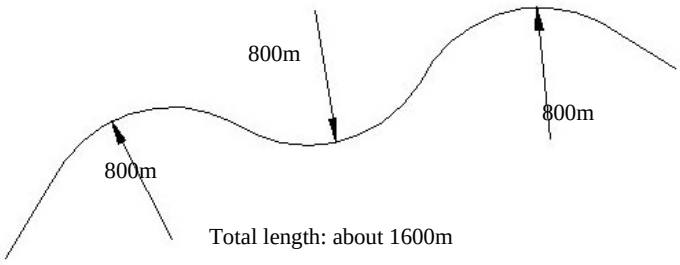

Figure 18. Path information used to test the lateral controller.

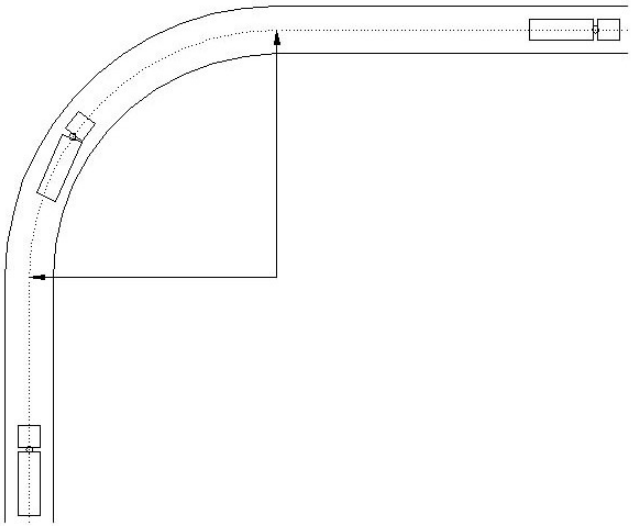

Figure 19. A HDV traveling along a curved path.

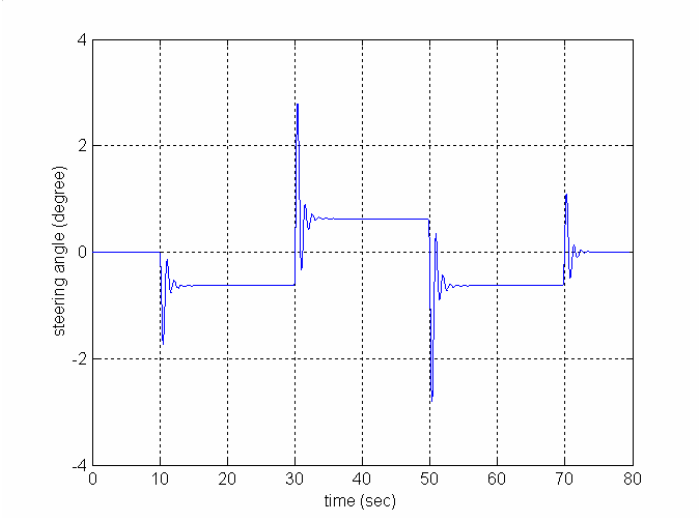

Figure 20. Steering angle response.

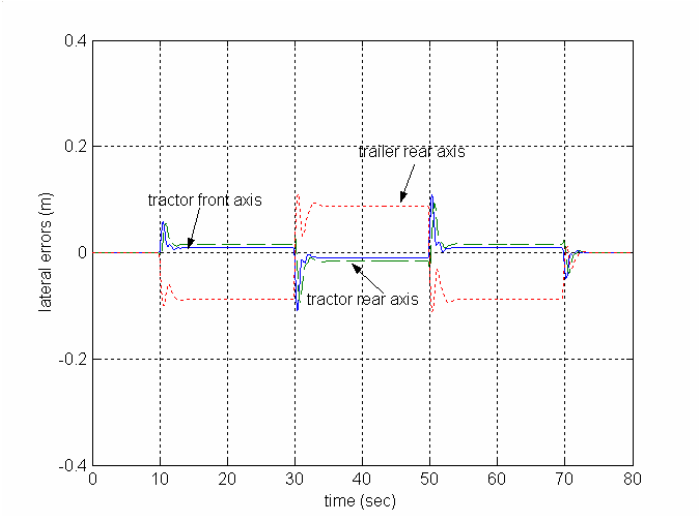

Figure 21. Lateral errors at the tractor front axis, rear axis and trailer rear axis.

The study in [8] has pointed out that there exists a large off-tracking error when the truck travels at a low speed around the curve. This situation needs more attention when the road curvature is large, i.e. the curve is sharp. As shown in Figure 22a, the truck might get off the center of the lane due to the large road curvature. To avoid this problem, we use a virtual offset for the road centerline denoted by the dashed line, tracking of which allows the truck to remain close to the actual centerline. Since each truck in the ACTIPOT system can be precisely located by the navigation system, it knows exactly the road curvature that lies ahead. Thus it is feasible to calculate the offset and "adjust" the road centerline. In the following simulations, adjustment for the road centerline will be employed when necessary. If the off-tracking cannot be compensated by the adjustment, increasing the lane width should be considered so that the automated trucks can follow the desired lane under a wide range of expected speeds without getting off the road.

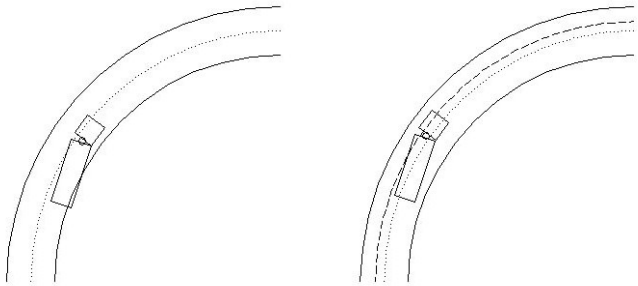

a b

Figure 22. Use of the virtual sensor offset method.

4 SUPERVISORY CONTROLLER

To organize the ACTIPOT system in an efficient and safe manner, a supervisory controller must be designed to dictate and synchronize the movements of the trucks and cranes. As shown in Figure 23, the supervisory controller is composed of two units: the Information Center and the Control Logic. All necessary information, such as path information, ship arrival and departure times, tasks to be performed and so on, are stored in advance in the Information Center. At the same time, every unit in the ACTIPOT system provides its updated status to the Information Center by direct communication. The Control Logic accesses the required information from the Information Center. In this report we focus on the control logic for the truck movement between the inland port and terminals. As shown in Figure 24, the supervisory controller assigns new tasks, checks truck positions, generates proper velocity trajectories and selects appropriate longitudinal/lateral controllers for the trucks under different situations.

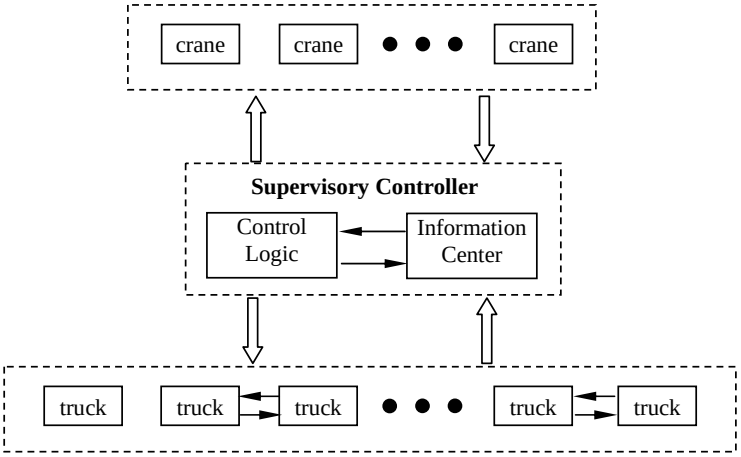

Figure 23. Interactions among the supervisory controller, trucks and cranes.

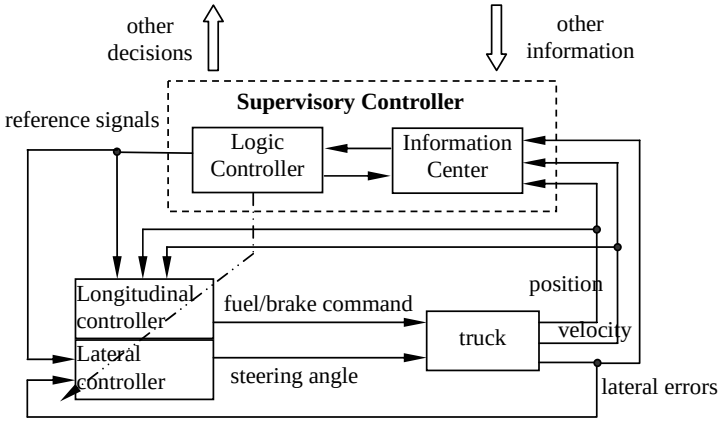

Figure 24. Interaction between the supervisory controller and a truck.

4.1 Control Logic

In the ACTIPOT system, a platoon with import containers slows down as it enters the inland port, checks which service lane is available, then splits so that the trucks operate in the individual mode. Individual trucks position themselves under the assigned cranes in the Import Buffer to get unloaded, move ahead, get loaded again under the assigned cranes in the Export Buffer, move toward PF and wait there until a platoon is formed. The new formed platoon moves at a low speed towards the exit of the inland port, speeds up to a desired velocity while cruising in the dedicated lanes, slows down to enter the container terminal, allows splitting of the trucks in such a way that the first truck in the platoon follows service lane 1 to access QC1, the second truck follows service lane 2 to access QC2 and so on. After being unloaded, a truck picks up another container and moves towards the PF to form the next platoon. The new platoon moves back to the inland port and the same process is repeated for all platoons.

In the ACTIPOT system, the basic requirement for the supervisory controller is to guarantee no collision, no congestion and good performance. The layout shown in Figure 5 and operations are designed for congestion-free environment. There are three collision possibilities between two trucks in the ACTIPOT system: when merging at the points P_1 or P_2 at the same time, when moving on different lanes due to lateral deviations and on the same lane due to unsafe intervehicle spacing. The first possibility has been automatically excluded by the two time windows T_1 and T_2 that time the merging so that no two trucks merge at the same time. The second possibility is eliminated too by designing robust lateral controllers that always keep the trucks very close to the center of the lane. The collision between two trucks traveling on the same lane is avoided by using intervehicle spacing that are safe under worst stopping and accelerating conditions. These considerations led to the following intervehicle spacing:

$$S_{safe} = \begin{cases} 6.6m, & v \le 8miles/hour \\ 1.2S_{stop}, & \text{otherwise} \end{cases} \quad (4\text{-}1)$$

where v is the truck velocity, S_{safe} is the safety spacing and S_{stop} is the stopping distance obtained from Figure 25 based on the simulated characteristics of the truck. Once a truck detects that there is another truck ahead on the same lane and the distance between them is less than S_{safe}, it will decelerate until the collision possibility disappears. Hence there will not be any collision occurring between two trucks on the same lane. Once the supervisory controller properly selects the longitudinal controllers and velocity trajectories, the system safety can be guaranteed, and there will be no deadlock in the system if the supervisory controller has no deadlock. This also tells us that the longitudinal behavior of the automated trucks is an important issue in the ACTIPOT system, and the longitudinal control logic is the most important part of the overall control logic.

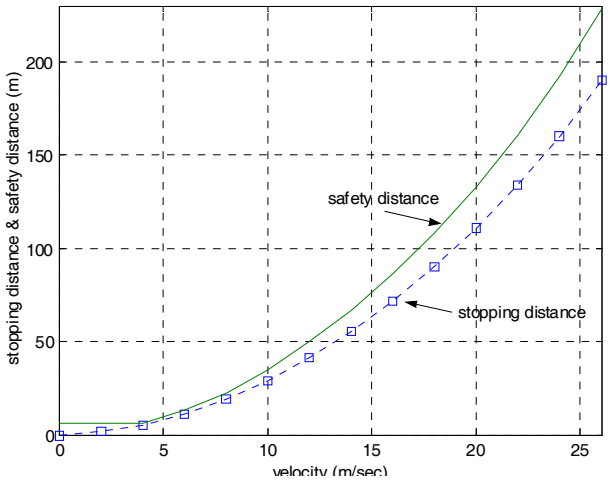

Figure 25. Stopping distance and safety distance.

According to the longitudinal velocity command, a truck in the autonomous mode is considered to have four states: acceleration, deceleration, cruise or stop. In the acceleration state, the supervisory controller generates an increasing speed signal. The desired acceleration is chosen to be 0.5m/s^2 if the truck speed is low, or 0.2m/s^2 if the truck speed is high. In the deceleration state, the supervisory controller generates a decreasing speed signal, which has an acceleration of -2m/s^2. In the cruising case, the truck follows a constant speed. In the stop state, the brake is always on so that the truck keeps still all the time. For a platoon, the leading truck is considered as operating in the autonomous mode, but the following trucks are considered as operating in the vehicle following mode.

4.2 Petri Net Modeling and Analysis

The use of Petri Nets is a graphic and mathematical modeling tool applicable to many systems. It is used in our report to model and analyze the properties of the supervisory controller. The Petri Net model of the supervisory controller consists of two sub-modules, one for trucks and one for cranes. We investigate the liveness and safeness properties of the modules individually and for the overall system. The basic definitions and theory of Petri Nets can be found in references such as [23], and will not be repeated here. Below we present the definitions and theorems that we use in our study.

Definition 4-1[23]: A *State Machine* (SM) is a Petri Net such that each transition t has exactly one input place and exactly one output place, i.e., $|{}^\bullet t| = |t^\bullet| = 1$ for all $t \in T$.

Definition 4-2[23]: A Petri Net is strongly connected if there exists a directed path from every node to every other node in $P \cup T$.

Theorem 4-1[23]: A state machine (N, M_0) is live iff N is strongly connected and M_0 has at least one token.

Theorem 4-2[23]: A state machine (N, M_0) is safe iff M_0 has at most one token. A live state machine (N, M_0) is safe iff M_0 has exactly one token.

It's easy to see that a live and safe state machine (N, M_0) is reversible, since a token that leaves a place can always go back to the same place.

4.2.1 Crane Modules

As shown in Figure 26, the control logic for a single-mode crane in the Import Buffer has four places:

1. *crane_idling*: no job is assigned to the crane, or the crane is ready to serve a truck but the truck has not arrived. A crane in this mode will keep idling until a job becomes available.
2. *unload_truck*: the crane unloads a container from a truck.
3. *move_container*: the crane moves the container towards the Import Buffer and stacks it.
4. *move_back*: the crane moves back for the next available job .

The transitions in this model are obvious, and the associated description is omitted.

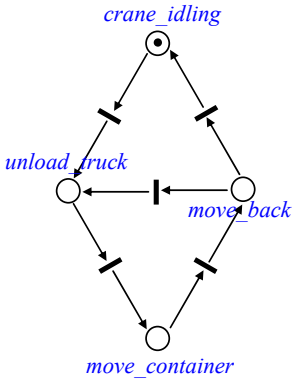

Figure 26. The module for a single-mode crane in the Import Buffer.

Similarly, the control logic for a single-mode crane in the Export Buffer is modeled in Figure 27. It also has four places:

1. *crane_idling*: this is the same as above.
2. *load_truck*: the crane loads a container onto a truck.
3. *move_back*: the crane moves towards the Export Buffer for the next container if available.
4: *move_container*: the crane moves a container from the Export Buffer to serve the arriving truck.

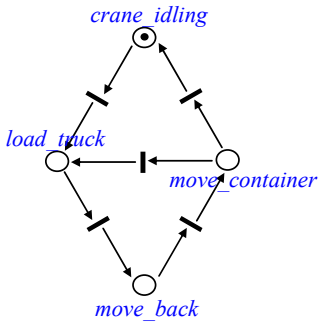

Figure 27. The module for a crane in the Export Buffer.

The control logic for a dual-mode quay crane is modeled in Figure 28. It has only two places:

1. *crane_idling*: the crane is waiting for the next coming truck.
2. *serve_truck*: the crane unloads an export container from the truck, moves it to the ship, stacks it, moves back with an import container and loads it onto the truck.

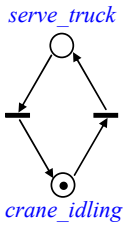

Figure 28. The module for a dual-mode quay crane in the container terminal.

It is easy to see that each of the three crane modules is strongly connected SM with only one token. Therefore, they are live, safe and reversible.

4.2.2 Truck Module

The control logic for an automated truck can be divided into three parts. As shown in Figure 29, they are "system check", "safety check" and "decision control". In fact, the control decisions, such as which on-board controllers to be used and what kind of velocity commands to be generated, are all decided by the key part "decision control". The first two parts are employed to assist "decision control", and will not generate any control decision directly. In other words, they can be implicitly included into the transitions of "decision control" as we will discuss below. The first part "system check" is used to check the functional status of the on-board systems and it has three places:

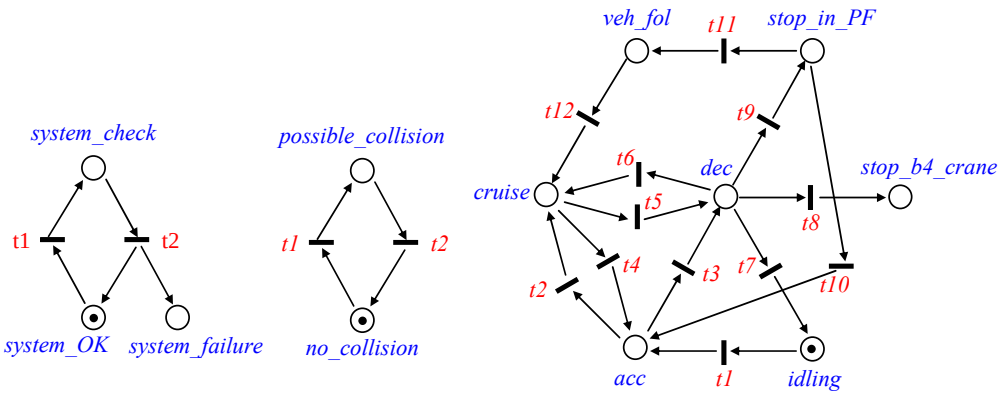

(a) system check **(b) safety check** **(c) decision control**

Figure 29. The module for an automated truck.

1. *system_OK*: A token is put in this place when all the on-board systems operate properly.

2. *system_check*: It is checking the on-board systems until all the containers have been transported. It is assumed that this check is almost instantaneous and introduces insignificant time delays.

3. *system_failure*: A token is put in this place once a system failure is detected.

The second part "safety check" incorporates the safety policy shown in Figure 29(b) into the supervisory controller, and it has two places:

1. *no_collision*: A token in this place indicates the safety policy is not violated, i.e., there is no collision possibility during the next time interval.

2. *possible_collision*: A token in this place indicates that the truck gets too close to another truck ahead and collision possibility exits if it keeps the current speed.

The third part, which is also the key part of the supervisory controller, is used to select appropriate controllers for trucks and provide reference signals if necessary. As shown in Figure 29(c), it has seven places and twelve transitions. The seven places in fact represent seven truck working states:

1. *idling*. The truck stays still in this state. This happens when the truck is waiting for others to join the platoon, or possible collision exists ahead or no job is assigned. The brake is always on during this state.

2. *acc*. The truck tracks a desired increasing speed trajectory and the longitudinal controller in (3-12) is engaged.

3. *cruise*. The truck tracks a constant speed and the controller in (3-12) is engaged.

4. *dec*. The truck tracks a decreasing speed trajectory and the controller in (3-12) is engaged.

5. *stop_b4_crane*. The truck stops before the assigned crane and waits until the service is complete. The brake is always on during this state.

6. *stop_in_PF*. The truck stops in PF and waits until the platoon is formed. The brake is always on during this state.

7. *veh_fol*. The truck is part of a platoon, but not a leader. In this case, it follows the preceding truck. The longitudinal controller in (3-47) is engaged.

The twelve transitions that represent different logic operations are:

1. *t1*. If the truck stops to avoid a possible collision, and that possible collision has vanished, then it will begin to accelerate.

2. *t2*. If the truck has reached the speed limit, then it will track that constant speed.

3. *t3*. If the truck detects a collision possibility during acceleration, it will slow down.

4. *t4*. If the truck has been cruising at a speed below the speed limit for some reason (we will come to this point at *t6*), and there is no collision possibility, then it will speed up.

5. *t5*. If the truck has detected a possible collision ahead or it needs to slow down to enter the service destination, it will decelerate until the collision possibility vanishes or it reaches the destination.

6. *t6*. If the truck decelerates because of possible collision and this collision possibility has vanished, then it will cruise at the current speed for a few seconds. During this cruising period, if the collision possibility reappears, then *t5* will take the truck back to *dec*. Otherwise, *t4* will transition the truck to the *acc*. There is no direct transition from *dec* to *acc*, because it may cause chattering.

7. *t7*. If a collision possibility exists during *dec*, then the truck will come to a complete stop.

8. *t8*. When the truck arrives at the service destination point, it will stop and wait there until it is served.

9. *t9*. When the truck enters the PF point, it will stop and wait until the platoon is formed.

10. *t10*. If the truck is the leading truck in a formed platoon, then it can transition to *acc* in a similar fashion as a truck in the autonomous mode.

11. *t11*. When the truck is within a formed platoon, then it will enter *veh_fol*.

12. *t12*. When the truck separates from a platoon, it will enter *cruise*.

As mentioned before, the sub-module "system check" has been incorporated into the transitions in "decision control". A token inside *system_OK* means any transition in "decision control" is possible, while a token inside *system_failure* forbids all transitions except *t3*, *t5* and *t7*. Thus the truck must come to a complete stop and wait to be towed away. A truck with system failure will be considered as a dead truck and must be removed from the ACTIPOT system. Since the dead truck will be removed from the system eventually, it can only affect system performance but not system liveness. Similarly, in "safety check", a token inside *possible_collision* will disable all the transitions except *t3*, *t5* and *t7*. But when the collision possibility disappears, the token will move back to *no_collision*, which will make all transitions valid again. In our analysis, we refer to the part "decision control" as the main control logic for trucks.

It is easy to see that the truck module is a state machine, but not live. It is not strongly connected since there is no path from *stop_b4_crane* to any other node. However, if the place *stop_b4_crane* and the transition *t8* are removed from the truck module, the left part is a strongly connected SM and contains only one token. Therefore it is live and safe.

4.2.3 Overall System

Although the truck module and the crane modules can be modeled and analyzed independently, they are not completely isolated. In the overall system, there is a "dynamic transition" between a truck and a crane, which dynamically links trucks and cranes together. This link exists only when the truck is under the service of the assigned crane, as shown in Figure 30. After the service is completed, this connection will automatically disappear. It can be seen that the dynamic transitions make the overall system live.

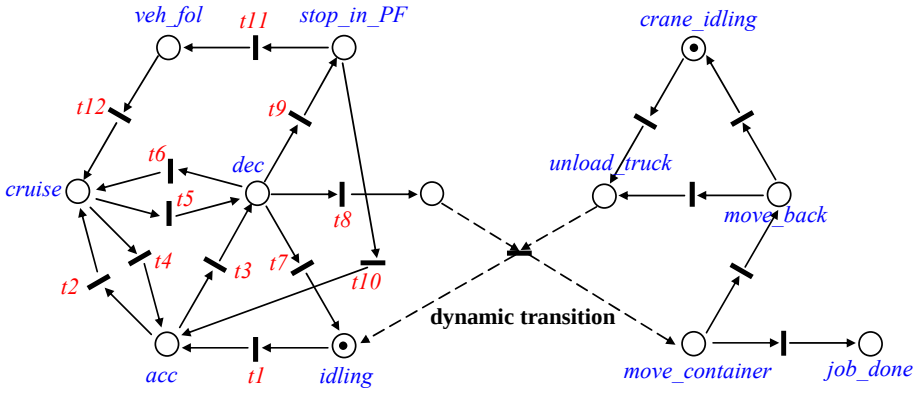

Figure 30. Dynamic transition between an automated truck and a single-mode crane.

Suppose the overall system is not live, i.e. there exists at least one deadlock in the overall system. Without loss of generality, this deadlock would correspond to one of the following three cases:

1. A token inside *system_failure* causes a deadlock for the truck. In this case, as soon as the system failure is detected, the truck comes to a stop and keeps idling. It may block the road in the ACTIPOT system and cause deadlock. However, the system liveness will recover once the failed truck is removed from the system.[†]

2. A deadlock exists inside the "decision control" module for an active truck. From the previous analysis, we know that this could only happen when a token in the place *stop_b4_crane* cannot move, which means that no crane is assigned to serve that truck. However, in our design, this is not possible as the five quay cranes are assigned to serve five service lanes respectively, and each truck can follow only one assigned lane. This is also true for the inland port, where the cranes serve the trucks on lane 1 and lane 2 alternatively, in a way that no truck is missed.

3. There is a deadlock in one crane module. From Figure 30, we can see that this deadlock may happen when there is no truck assigned to that crane. Since we have designed the service lanes so that any crane is accessible to any truck in the system, no truck assigned to the crane means the crane has broken down or the path to it is blocked for emergency. However, it will not affect the liveness of the whole system since the other cranes still work. Once we properly revise the dispatching rule so that all the trucks are assigned only to the active cranes, the system is still live. This point is verified using microscopic simulations, where a crane that cannot work properly is simulated.

Given the above discussions we can conclude that the overall system is live. As shown in Figure 31, the supervisory controller can be viewed as a collection of relatively independent sub-modules connected by the dynamical transitions. Furthermore, since a

[†] Due to budget and time constraints, the study of possible failures, their detection and accommodation has not been pursued under this project.

token in the overall system is always inside one sub-module, the Petri Net model for the overall system is safe.

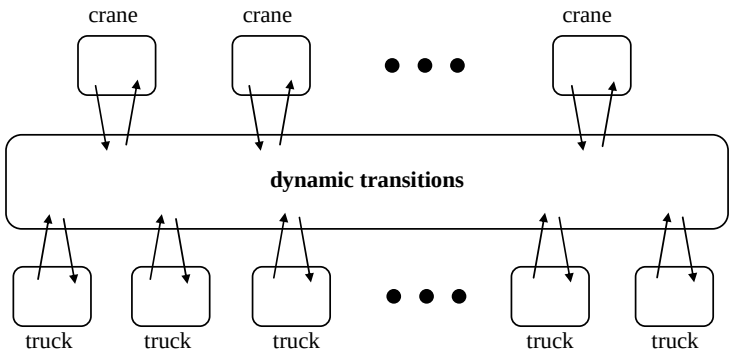

Figure 31. Overview of the supervisory controller.

4.3 Simulations

Using the developed supervisory, longitudinal and lateral controllers, we study the behavior of one platoon employed in the ACTIPOT system, which has the layout in Figure 5. The platoon, composed of 5 trucks, speeds up to 20.1m/s (about 45 miles per hour) after leaving the inland port, cruises with this speed towards the container terminal, and slows down to 3.6 m/s (8 miles per hour) to enter the container terminal. The velocity, relative velocity, separation distance and separation error responses are shown in Figure 32, 33, 34 and 35, respectively. In each figure, all the responses overlap together since the time scale is large, which also indicates that the whole platoon can be viewed as one unit. Since safety and absence of collision between trucks is an important concern in the ACTIPOT system, we should pay more attention to the separation distances. Figure 34 shows that the separation distance between any two adjacent trucks is larger than 2.8m even in the worst case, indicating a collision-free operation. The travel distance and steering angle responses of the five trucks are shown in Figure 36 and 37. Figures 38, 39 and 40 indicate that the lateral errors are always kept much less than 0.4m, which means that the trucks are kept within the dedicated lanes so that no collision could happen between two units operating on different lanes.

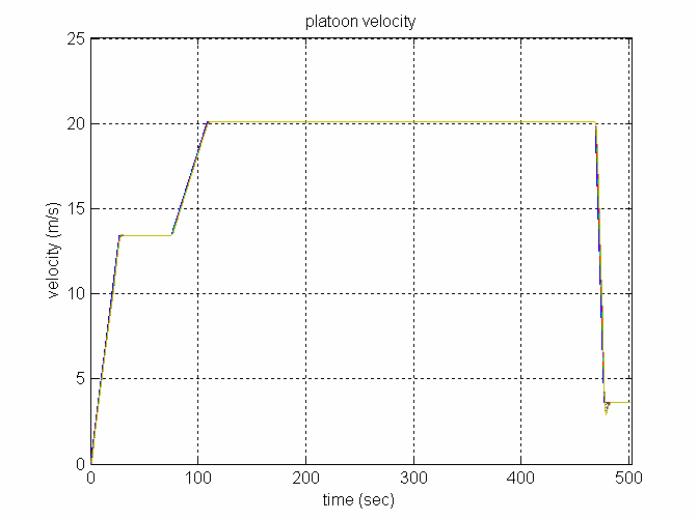

Figure 32. Velocity responses of the five trucks in the platoon.

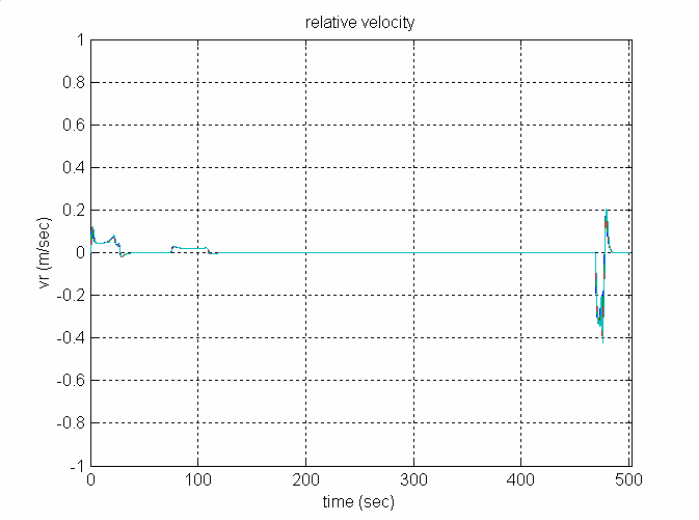

Figure 33. Relative velocity responses of two vehicles in the platoon.

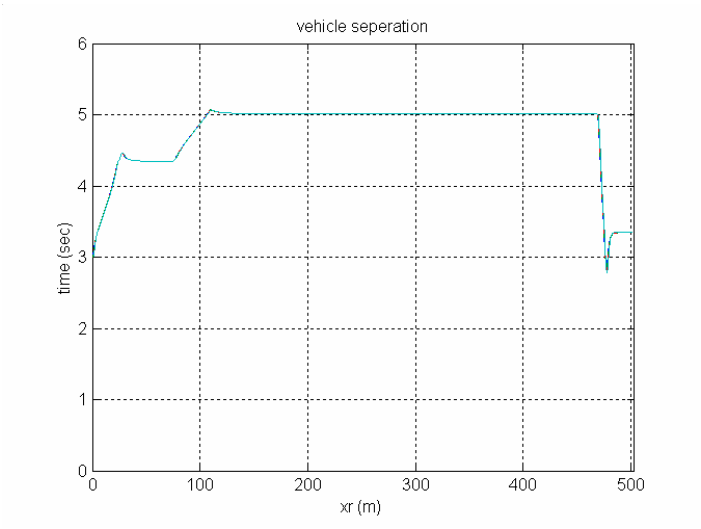

Figure 34. Separation distance responses in the platoon.

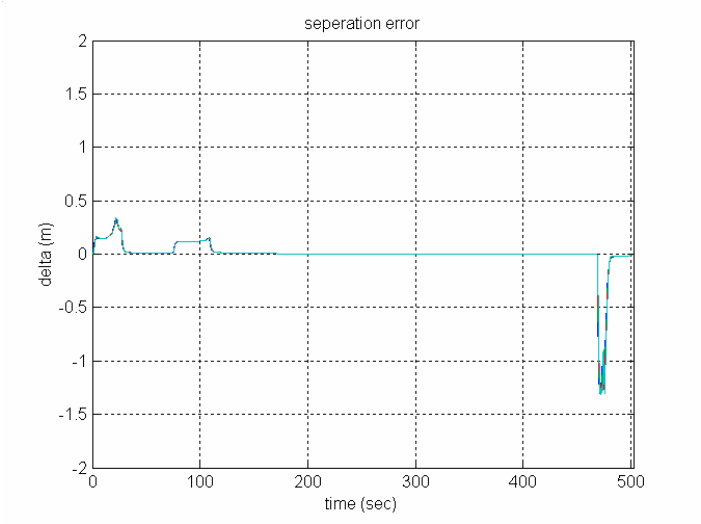

Figure 35. Separation error responses in the platoon.

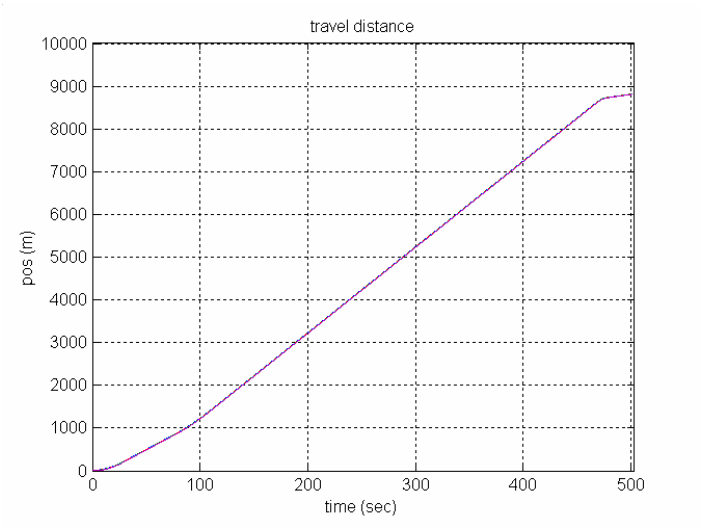

Figure 36. Truck travel distances.

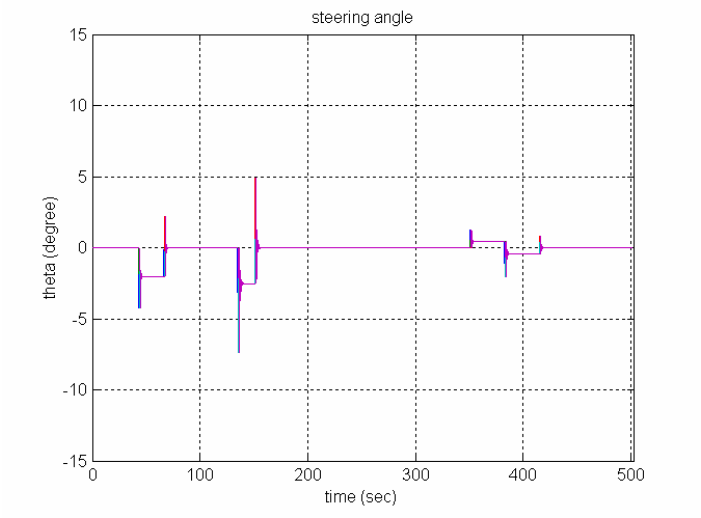

Figure 37. The steering angles of five vehicles in the platoon.

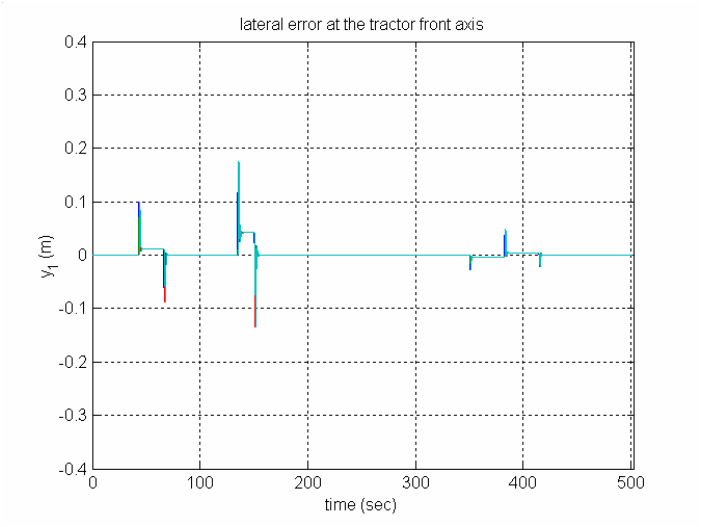

Figure 38. The lateral errors at the tractor front axes.

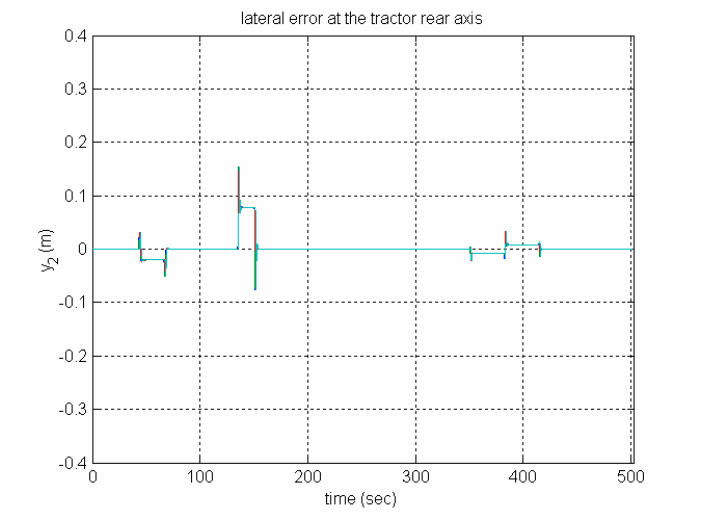

Figure 39. The lateral errors at the tractor rear axes.

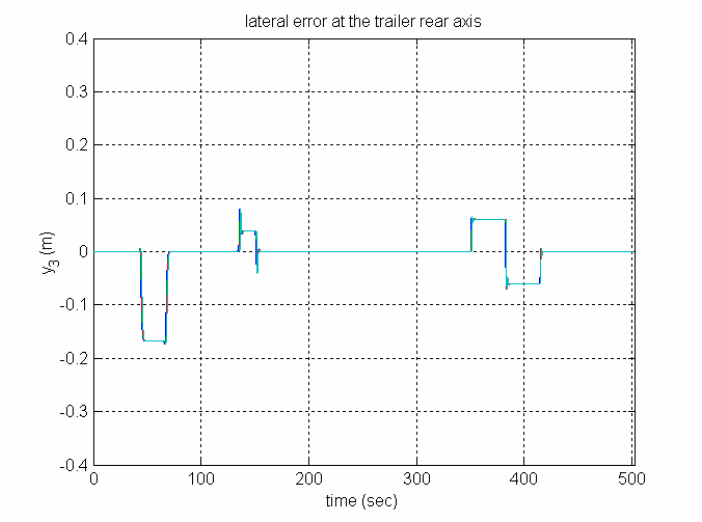

Figure 40. The lateral errors at the trailer rear axes.

The operation an individual truck within the container terminal and inland port has also been simulated. Here, we only present the simulation results of a truck traveling in the container terminal. The simulation assumes that after the truck is released from a platoon, it follows the service lane 1, cruises at a speed of 3.6 m/s towards the assigned crane, stops at the assigned point under the crane and waits until it is served. It then moves to the PF point and waits for a platoon formation. The velocity response and travel distance are shown in Figure 41 and 42. Also, from Figure 44, 45 and 46, we can see that the lateral errors are much smaller than 0.4m, indicating that the truck remains close to the center of the assigned lane.

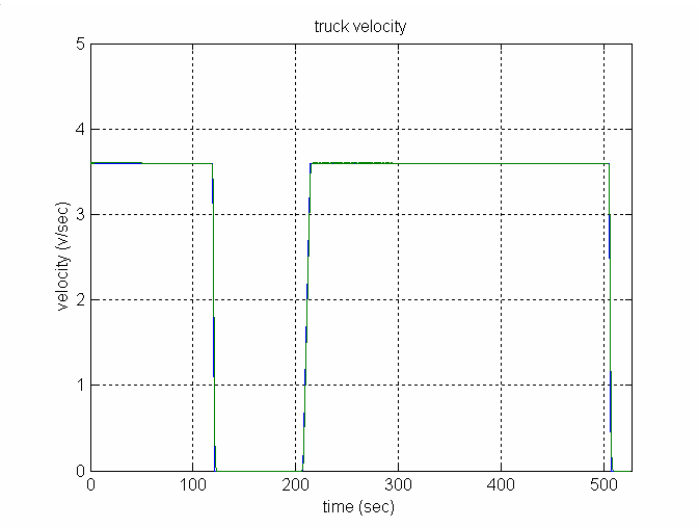

Figure 41. The velocity response of the truck.

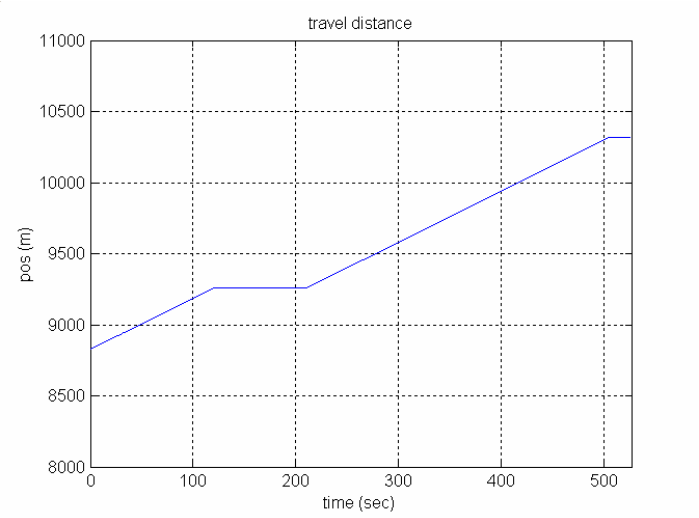

Figure 42. Truck travel distance.

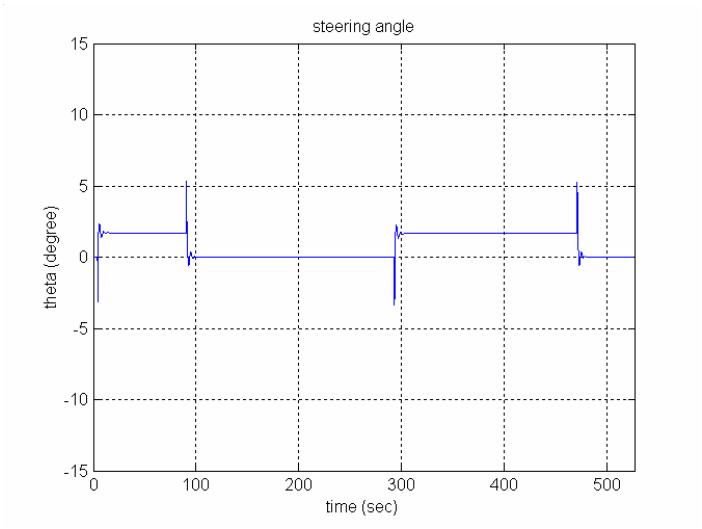

Figure 43. The steering angle of the truck.

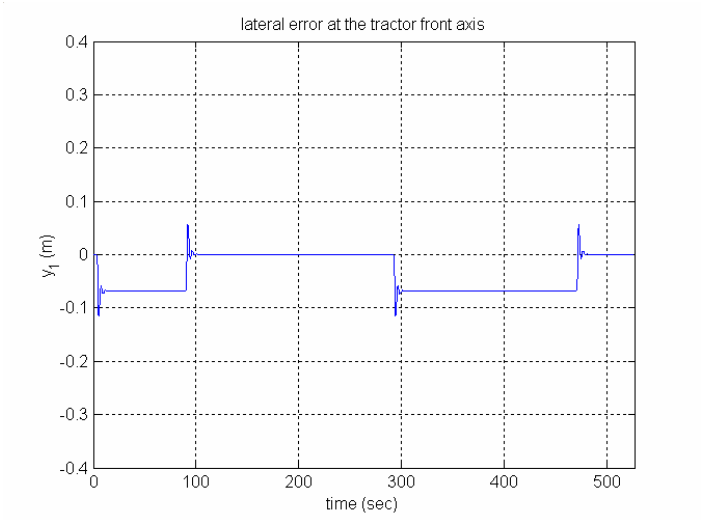

Figure 44. The lateral error at the tractor front axis.

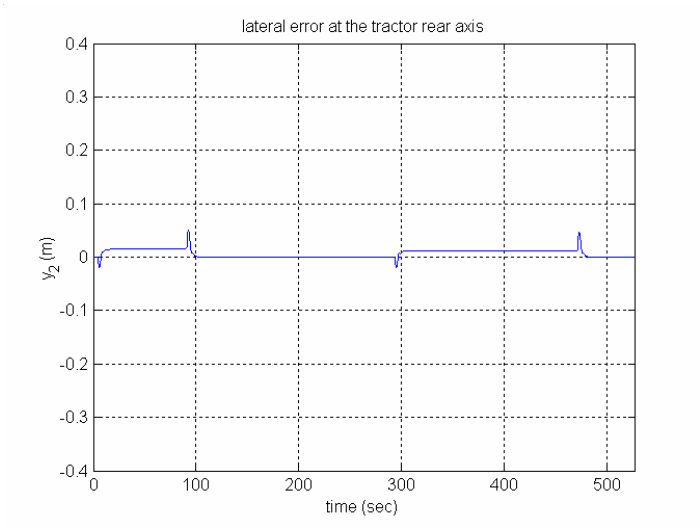

Figure 45. The lateral error at the tractor rear axis.

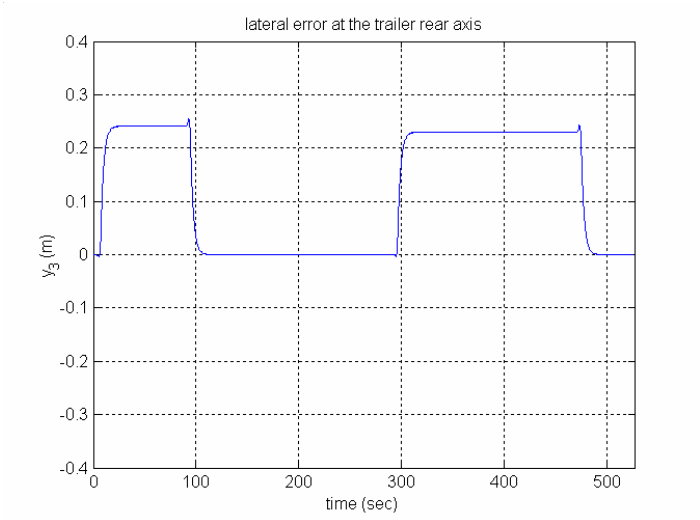

Figure 46. The lateral error at the trailer rear axis.

The above two illustrative simulations demonstrate how the supervisory controller operates with respect to one platoon or truck. The next step is to demonstrate that the supervisory controller guarantees the safety and efficiency of the ACTIPOT system involving a large number of automated trucks.

5 SIMULATIONS AND ANALYSIS OF THE ACTIPOT SYSTEM

In order to simulate the overall performance of the ACTIPOT system, the dynamics of the controlled trucks should be further simplified in order to reduce the system complexity. The simulations for individual platoons and trucks discussed above demonstrate that the trucks can always be kept within the dedicated lanes without colliding or getting off the assigned lane or position. Since the lateral behavior of a truck has little effect on the truck traveling time, the lateral truck dynamics are neglected in order to reduce the number of computations further. Another simplification is to approximate the longitudinal dynamics of the truck with the simple equation

$$v(t) = v_d(t - \tau_1) \tag{5-1}$$

where $v(t)$ is the longitudinal velocity of the truck, $v_d(t)$ is the desired velocity and the time delay τ_1 is selected to be a positive number. Since the string stability can be guaranteed by the proposed control law in (3-47), the longitudinal behavior of a platoon is viewed as an individual truck with larger length. We use the Matlab Stateflow toolbox for simulations. The simplified truck model (5-1) and the control logic presented in section 4.2 are used.

In the proposed ACTIPOT system, the truck turnaround time T_{truck} is defined as the average time for one truck to transport one container from the inland port to the container terminal and transport another one back to the inland port when there is no traffic congestion. To make the ship turnaround time limited by T_{ship}, the required number of trucks is obtained from

$$\underline{N}_{truck} = \left\lceil \frac{N_{container} T_{truck}}{T_{ship}} \right\rceil \tag{5-2}$$

Another way to determine the number of needed trucks is to keep the quay cranes as busy as possible, which provides the required truck number as

$$\overline{N}_{truck} = \lceil N_{qc} C_{qc} T_{truck} \rceil \tag{5-3}$$

Given the number of the cranes N_{qc} provided by (2-1), it can be seen that $\overline{N}_{truck}$ is not less than $\underline{N}_{truck}$. It is desired to keep the number of trucks as small as possible in order to minimize cost and reduce the possibility of truck traffic congestion. On the other hand, a small number of trucks may increase the idling time of the quay cranes and reduce the terminal throughput. In our study, the number of trucks is varied between $\underline{N}_{truck}$ and $\overline{N}_{truck}$, and its effect on the overall performance is studied.

The efficiency of the *i*th quay crane can be evaluated by its busy rate $BR_{qc}(i)$, which is defined as

$$BR_{qc}(i) = \frac{Busy\ Period(i)}{Busy\ Period(i) + Idle\ Period(i)} \tag{5-4}$$

where *Busy Period (i)* represents the total time that the *i*th quay crane is engaged for loading/unloading trucks, and *Idle Period (i)* is the total time that the *i*th quay crane is not engaged in any job. The average busy rate of the quay cranes BR_{qc} is defined as

$$BR_{qc} = \frac{1}{N_{qc}} \sum_{i=1}^{N_{qc}} BR_{qc}(i) \tag{5-5}$$

The average busy rate of the cranes in the inland port BR_{pc} is defined in the same manner as (5-4) and (5-5). The efficiency of the trucks can be similarly evaluated by their average busy rate BR_{truck}, defined as

$$BR_{truck} = \frac{N_{container} T_{truck}}{N_{truck} T_{system}} \tag{5-6}$$

where T_{system} is the total time for the ACTIPOT system to accomplish the assigned transportation task. If the ACTIPOT system is designed properly, the busy rates of the quay cranes and trucks should be high and the ship turnaround time should be within the desired time window.

5.1 Case 1

In this case, the ACTIPOT system shown in Figure 5 is simulated with the system description given in section 2.1. From the completed simulation results in section 4.3, we know that the truck turnaround time T_{truck} is about 1464 seconds, and $\underline{N}_{truck}$ is 70 and $\overline{N}_{truck}$ is 86. Therefore, the optimal number of trucks should stay between these two numbers. The simulation results are shown Figure 47. When 80 trucks are employed in the ACTIPOT system, the ship turnaround time is close to the minimum value and the quay crane busy rate is kept close to its maximum value. At the same time, the traffic congestion is not serious since the truck busy rate is close to 1. Increasing the number of trucks beyond 80, the ship turnaround time does not decrease significantly, but the traffic congestion becomes more and more serious, which means the system efficiency is decreasing. Decreasing the number of trucks below 80 increases the ship turnaround time and reduces the busy rate of the quay cranes. All these results indicate that the optimum number of trucks for such a system is close to 80. It should be noted that BR_{qc} can not

get too close to 1, because it takes some time for a truck to position itself under the cranes, which means a quay cranes in the dual mode has to idle during that period.

With the truck number fixed to be 80, similar simulations are performed for ships with different load ratios and shown in Figure 48. It is clear that there is a linear relation between ship turnaround time and the ratio of shipload to ship capacity, which indicates that the system performance is insensitive to crane uncertainties.

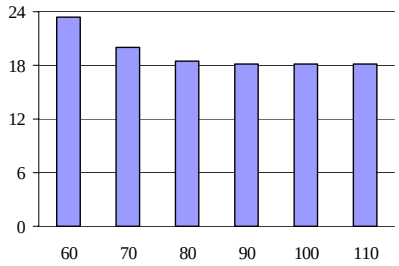

(a) ship turnaround time (hours) vs. truck number.

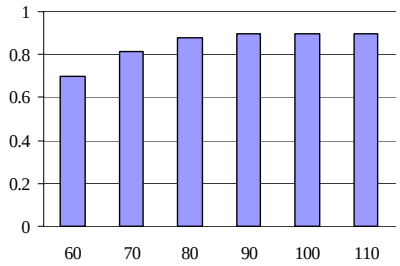

(b) quay crane busy rate vs. truck number

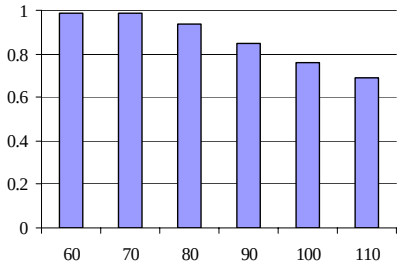

(c) truck busy rate vs. truck number.

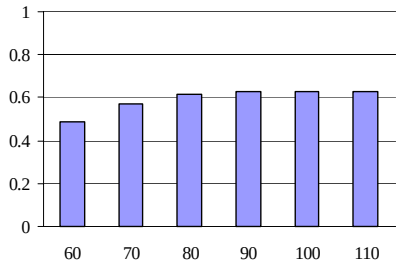

(d) port crane busy rate vs. truck number

Figure 47. Simulation results for case 1.

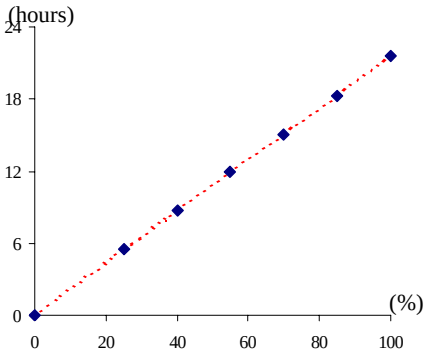

Figure 48. Ship turnaround time vs. container quantity.

Let us now consider some emergency cases. Suppose an automated truck breaks down for some reason and it will take 20 minutes to clear the failed truck and for the system to recover. Further assume that the ship carries 4000 FEUs and 80 trucks are employed. The following scenario have been simulated:

1. The truck breaks down in a service lane in the terminal and causes the service lane to close down leaving only four ship cranes to carry out the loading/unloading operations while the fifth crane idles for about twenty minutes. A backup truck is released to the system after the failed truck is removed, thus there are still 80 trucks available. The dispatching rule for trucks is temporarily modified so that each truck moves towards a crane with the least number of waiting trucks after been released from the platoon. Simulation of this scenario shows that the ship turnaround time is near 21.7 hours. Compared with the turnaround time in the normal case of 21.6 hours, the broken truck has caused only 0.1 hours difference.

2. The truck breaks down in the dedicated lanes between the inland port and the terminal, blocking the lane and creating congestion. In this case, simulations shows the ship turnaround time becomes about 22.0 hours, which means the 20 minutes lost cannot be compensated.

5.2 Case 2

This simulation considers a loading-only case for the ship. In the ACTIPOT system with a layout shown in Figure 5, it is required to load an empty ship to its 85% capacity. The quay cranes will work in the single mode, and in this case the truck turnaround time is about 1388 seconds. From (5-2) and (5-3), we know that the optimum number of trucks lies between 66 and 97. This point can be verified by the simulation results shown in Figure 49. As we can see, 70 trucks are enough to make the ship turnaround time less than 20 hours, while 100 trucks are required to squeeze the quay cranes to their busiest mode. Note BR_{qc} can almost reach 1 in this case because all the quay cranes work in the single mode, thus the time spend to position the truck under the crane does not affect the speed of the crane. At the same time, the trucks work in an efficient manner when less than 100 trucks are employed. Similar results can be obtained if we consider the unload-only case.

5.3 Case 3

In the third case, we modify Figure 5 so that the inland port has the same layout as the container terminal, thus the ACTIPOT system is almost symmetric. With the truck turnaround time 1590 seconds, we have $\underline{N}_{truck}$ = 76 and $\overline{N}_{truck}$ = 93. The simulation results in Figure 50 show that 80 or more trucks are needed to accomplish the transportation task within 20 hours, and the optimum number of trucks is between 80 and 90.

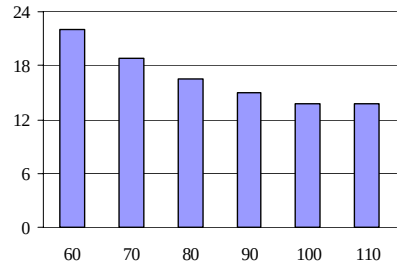

(a) ship turnaround time (hours) vs. truck number.

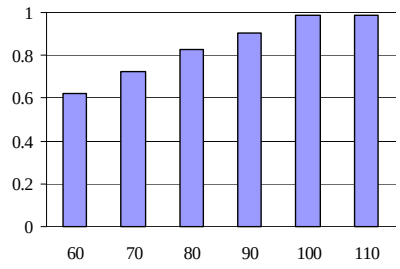

(b) quay crane busy rate vs. truck number

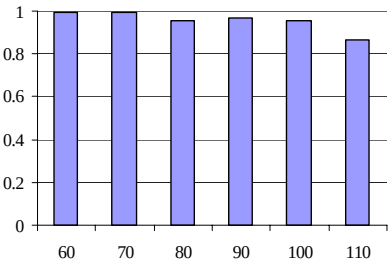

(c) truck busy rate vs. truck number.

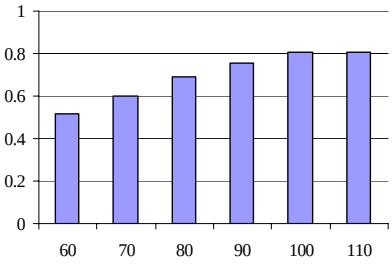

(d) import crane busy rate vs. truck number

Figure 49. Simulation results for case 2.

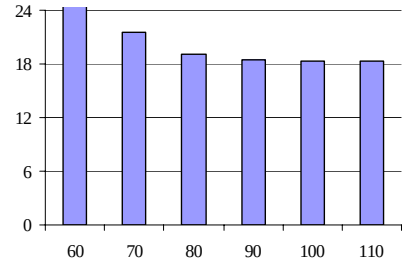

(a) ship turnaround time (hours) vs. truck number.

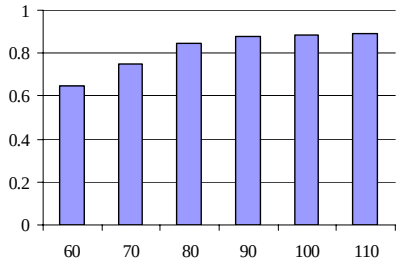

(b) quay crane busy rate vs. truck number

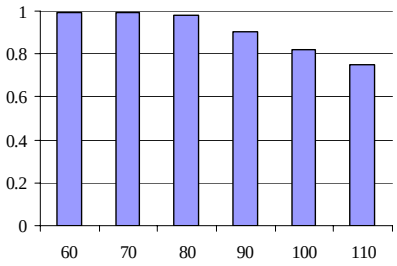

(c) truck busy rate vs. truck number.

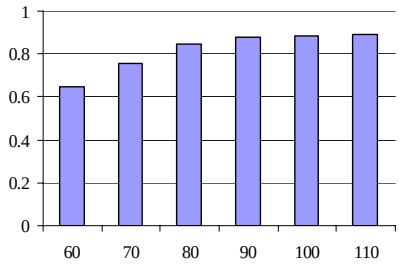

(d) port crane busy rate vs. truck number

Figure 50. Simulation results for case 3.

The above simulations, demonstrate that the ACTIPOT system operates as designed during normal operations. It can also accommodate failures in an effective way without significantly affecting performance where possible.

6 CONCLUSION

In this study we propose a new concept called “Automated Cargo Transportation system between Inland POrt and Terminals” (ACTIPOT) which involves the use of automated trucks to transfer containers from an inland port to terminals. The inland port could be a few or more miles away from the terminals where lower cost land is available and is used for storing and processing import/export containers before distribution to customers or transfer to the terminal for loading on ships.

In this report, we design, analyze, simulate and evaluate the various components of the ACTIPOT system with emphasis on the lateral and longitudinal control of the automated trucks and on the overall supervisory controller that synchronizes all operations and transfer of containers between the terminal and inland port using dedicated truck lanes. We employ the use of truck platoons in order to make the control of the overall system easier to handle and understand therefore minimizing the possibility of deadlocks, congestion and failures. Simulations are used to demonstrate that each subsystem operates in a satisfactory manner. Larger scale microscopic simulations are performed to demonstrate the overall performance of the ACTIPOT system. The choice of distances and other variables in the ACTIPOT system are selected by using the ICTF facility as the inland port and Pier G as the terminal both located in the Long Beach area.

Our preliminary study indicates that the ACTIPOT system is feasible and could operate in an efficient manner. The issues that require further investigation are cost analysis and effectiveness as well as acceptance by terminals and other stakeholders. Furthermore technical issues such as particular choices of sensors, actuators, equipments based on cost, reliability and performance considerations need to be addressed by performing actual experiments and additional studies. Another important issue is the location of the ACTIPOT system and the availability of land for an inland port and of dedicated lanes to connect the inland port with the terminals.

IMPLEMENTATION

The results of this project demonstrate that the implementation of the proposed ACTIPOT system will alleviate the pressure terminals are facing for additional land to be used for container storage and operations. The technologies required for implementation of the ACTIPOT system, such as sensors, control algorithms, communication and navigation, are currently available, which make the implementation of the system from the technology point of view feasible. One possible site for implementation is the Long Beach area where some variables such as distances and geometry of road system are used in our simulations of the ACTIPOT system.

The issues that require further investigation are cost analysis and effectiveness as well as acceptance by terminals and other stakeholders. Furthermore technical issues such as particular choices of sensors, actuators, equipments based on cost, reliability and performance considerations need to be addressed by performing actual experiments and additional studies. Another important issue is the location of the ACTIPOT system and the availability of land for an inland port and of dedicated lanes to connect the inland port with the terminals.

APPENDIX A: Notations

c_a aerodynamic drag coefficient
c_r rolling friction coefficient
d_1, d_2 relative position (x, y) between tractor's CG and the fifth wheel (m)
d_3, d_4 relative position (x, y) between semi-trailer's CG and the fifth wheel (m)
C_{af} cornering stiffness of the tractor front tires (N/rad)
C_{ar} cornering stiffness of the tractor rear tires (N/rad)
C_{at} cornering stiffness of the semi-trailer tires (N/rad)
F_t tractive tire force (N)
F_a aerodynamic drag force (N)
F_r rolling friction force (N)
h_w radius of the front wheels (m)
I_{z1} tractor yaw moment of inertia (kg m^2)
I_{z2} semitrailer yaw moment of inertia (kg m^2)
J_e effective inertia of the engine (kg m^2)
J_{tc} effective inertia of the turbocharger (kg m^2)
J_w effective inertia of the front wheels (kg m^2)
k_t empirically determined constant (for tractive tire force)
l_1 distance between tractor CG and front wheel axle (m)
l_2 distance between tractor CG and rear wheel axle (m)
m truck mass ($m_1 + m_2$) (kg)
m_1 tractor mass (nominal value 7700kg)
m_2 trailer and cargo mass (nominal value 15000kg)
$\dot{m}_c$ compressor air mass flow rate (kg/sec)
M_b brake torque (N m)
M_{bc} commanded brake torque (N m)
M_c torque absorbed by the compressor (N m)
M_f engine friction torque (N m)
M_{ind} engine indicated torque (N m)
M_{load} engine load torque (N m)
M_t torque generated by the turbine in TC (N m)
M_P torque converter pump torque (N m)
M_T turbine torque in the automatic transmission (N m)
N_e engine speed (rpm)
R gas constant (kJ/kg K)
R_i reduction ratio of the *i*th gear

R_d final drive reduction ratio

T_{im} intake manifold temperature (K)

v truck velocity (m/sec)

v_d desired truck velocity (m/sec)

v_r relative velocity (m/sec)

V_d engine displacement volume (m^3)

V_{im} intake manifold volume (m^3)

$\dot{x}_u$ longitudinal speed of the tractor along the unsprung mass coordinate (m/sec)

x_r separation distance (m)

y_u lateral displacement of tractor's CG with respect to the unsprung mass frame (m/sec)

y_r lateral displacement of tractor's CG with respect to the road center line (m/sec)

Y fueling index (or rack position) (m)

α_i , β_i polynomial coefficients i =0, 1, 2

ε_1 yaw angle of the tractor with respect to inertial frame (rad)

ε_f relative yaw angle between the tractor and the semitrailer (rad)

ε_r yaw angle of the tractor relative to the road center line (rad)

$\dot{\varepsilon}_d$ desired yaw rate set by the curved road ($\dot{\varepsilon}_d = v/\rho$) (rad/sec)

δ separation error (m)

η_v volumetric efficiency

μ road adhesion coefficient (nominal value 0.8)

ρ road curvature (m)

τ_b approximated brake time constant (sec)

τ_i average time delay of the engine torque (sec)

θ_s angle of the steering wheel (rad)

θ_w angle of the front wheels (rad)

ω_e engine speed (rad/sec)

ω_{tc} turbocharger rotor speed (rad/sec)

ω_w angular velocity of the driving wheels (rad/sec)

ω_P pump speed (assumed to be equal to the engine speed) (rad/sec)

ω_T turbine speed (rad/sec)

APPENDIX B: Longitudinal Model

The complete longitudinal dynamics of a HDV involves the diesel engine, the automatic transmission and the drivetrain. The turbocharged diesel engine is described by three differential and several algebraic equations. Only the three differential equations are presented here. The three states are the intake manifold (IM) pressure p_{im}, the engine speed ω_e and the Turbocharger (TC) rotor speed w_{tc}. The intake manifold pressure can be described as

$$\dot{p}_{im} + \frac{\eta_v V_d N_e}{120 V_{im}} p_{im} = \dot{m}_c \frac{R T_{im}}{V_{im}} \tag{B-1}$$

where T_{im} and V_{im} are respectively the IM temperature and volume, η_v is the volumetric efficiency, V_d is the displacement of the engine, N_e is the engine speed and $\dot{m}_c$ is the compressor air mass flow rate. The differential equation for the engine speed is

$$J_e \dot{\omega}_e = M_{ind}(t - \tau_i) - M_f(t) - M_{load}(t) \tag{B-2}$$

where M_{ind} is the indicated torque, M_f is the friction torque of the engine, M_{load} is the load torque, J_e is the effective inertia of the engine, and τ_i is the average difference between the time of issuing a command to change the indicated engine torque and the time when the injection valve can be operated. The TC rotor speed is described as

$$\dot{\omega}_{tc} = \left(M_t - M_c\right) / J_{tc} \tag{B-3}$$

where M_t is the torque provided by the turbine, M_c is the torque absorbed by the compressor, and J_{tc} is the effective inertia of the turbocharger. The fuel command u_f has been included in the algebraic equations of calculating M_{ind}.

The automatic transmission model is obtained under the assumptions that the gear shift is instantaneous and that there is no torsion in the driveline. The torque converter is modeled approximately as

$$\begin{cases} M_P = \alpha_0 \omega_P{}^2 + \alpha_1 \omega_P \omega_T + \alpha_2 \omega_T{}^2 \\ M_T = \beta_0 \omega_P{}^2 + \beta_1 \omega_P \omega_T + \beta_2 \omega_T \end{cases} \tag{B-4}$$

where M_P is the pump torque, M_T is the turbine torque, ω_P is the pump speed and assumed to be equal to the engine speed, ω_T is the turbine speed, and the coefficients α_i and β_i (i=1,2 and 3) are obtained from experimental data. Furthermore, the assumption that there is no torsion in the driveline establishes a direct relation between the angular velocity of the torque converter turbine ω_T and that of the vehicle's driving wheels ω_w:

$$\omega_w = R_i R_d \omega_T = R_{total} \omega_T \tag{B-5}$$

where R_i is the reduction ratio of the *i*th gear and R_d is the final drive reduction ratio.

In the longitudinal drivetrain model, the angular velocity of the driving wheels ω_w is determined by the torque converter turbine torque M_T, the tractive tire torque $F_t h_w$ and the brake torque M_b

$$J_w \dot{\omega}_w = \frac{M_T}{R_{total}} - F_t h_w - M_b \tag{B-6}$$

The brake dynamics is approximated as a first-order linear system

$$\dot{M}_b = \frac{M_{bc} - M_b}{\tau_b} \tag{B-7}$$

where M_{bc} is the commanded brake torque and τ_b is the approximated brake time constant. The tractive tire force F_t depends linearly on the tire slip up to 15% slip, and it is represented by

$$F_t = \begin{cases} k_t \left(1 - \dfrac{v}{h_w \omega_w}\right) & if\ h_w \omega_w \geq v \\ -k_t \left(1 - \dfrac{h_w \omega_w}{v}\right) & if\ h_w \omega_w < v \end{cases} \tag{B-8}$$

where k_t is a coefficient determined by experiments. The state equation for the truck velocity is

$$\dot{v} = \frac{F_t - F_a - F_r}{m} \tag{B-9}$$

where m is the vehicle mass, F_a is the aerodynamic drag force, and F_r is the rolling friction force. In (B-9),

$$\begin{cases} F_a = c_a v^2 \\ F_r = \dfrac{c_r m g}{h_w} \end{cases} \tag{B-10}$$

where c_a is the aerodynamic drag coefficient, c_r is the rolling friction coefficient, h_w is the radius of the front wheels, g is the gravity constant, and the brake/fuel commands are incorporated in the differential and algebraic equations that determine the tractive tire force F_t. The two constants, c_a and c_r, are achieved in experiment.

More detailed information about the nonlinear longitudinal model can be found in [9, 13].

APPENDIX C: Lateral Model

The lateral model is developed with respect to the unsprung mass reference frame under the following assumptions:

1. The roll motion is small enough to be neglected.
2. The longitudinal acceleration $\ddot{x}_u$ is small.
3. Tire slip angles of the left and the right wheels are the same.
4. Tire longitudinal and lateral forces are represented by the linearized tire model.

The lateral model of the tractor-semitrailer vehicles is

$$M\ddot{q} + C(q,\dot{q}) + D\dot{q} + Kq = F\theta_w \tag{C-1}$$

where q is the generalized coordinate vector

$$q = \begin{bmatrix} y_u & \varepsilon_1 & \varepsilon_f \end{bmatrix}^T$$

M is the inertia matrix,

$$M = \begin{bmatrix} m_1 + m_2 & -m_2(d_1 + d_3\cos\varepsilon_f) & -m_2 d_3\cos\varepsilon_f \\ -m_2(d_1 + d_3\cos\varepsilon_f) & I_{z1} + I_{z2} + m_2(d_1^2 + d_3^2) + 2m_2 d_1 d_3\cos\varepsilon_f & I_{z2} + m_2 d_3^2 + m_2 d_1 d_3\cos\varepsilon_f \\ -m_2 d_3\cos\varepsilon_f & I_{z2} + m_2 d_3^2 + m_2 d_1 d_3\cos\varepsilon_f & I_{z2} + m_2 d_3^2 \end{bmatrix}$$

$C(q,\dot{q})$ is the vector of Coriolis and Centrifugal forces,

$$C(q,\dot{q}) = \begin{pmatrix} (m_1 + m_2)\dot{x}_u\dot{\varepsilon}_1 + m_2 d_3\sin\varepsilon_f(\dot{\varepsilon}_1 + \dot{\varepsilon}_f)^2 \\ -m_2(d_1 + d_3\cos\varepsilon_f)\dot{x}_u\dot{\varepsilon}_1 - m_2 d_3\sin\varepsilon_f\dot{y}_u\dot{\varepsilon}_1 - 2m_2 d_1 d_3\sin\varepsilon_f\dot{\varepsilon}_1\dot{\varepsilon}_f - m_2 d_1 d_3\sin\varepsilon_f\dot{\varepsilon}_f \\ -m_2 d_3\sin\varepsilon_f\dot{y}_u\dot{\varepsilon}_1 - m_2 d_3\cos\varepsilon_f\dot{x}_u\dot{\varepsilon}_1 + m_2 d_1 d_3\sin\varepsilon_f\dot{\varepsilon} \end{pmatrix}$$

D is the damping matrix,

$$D = \frac{2}{\dot{x}_u}\begin{bmatrix} C_{\alpha_f} + C_{\alpha_r} + C_{\alpha_t} & l_1 C_{\alpha_f} - l_2 C_{\alpha_r} - (l_3 + d_1)C_{\alpha_t} & -l_3 C_{\alpha_t} \\ l_1 C_{\alpha_f} - l_2 C_{\alpha_r} - (l_3 + d_1)C_{\alpha_t} & l_1^2 C_{\alpha_f} + l_2^2 C_{\alpha_r} + (l_3 + d_1)^2 C_{\alpha_t} & l_3(l_3 + d_1)C_{\alpha_t} \\ -l_3 C_{\alpha_t} & l_3(l_3 + d_1)C_{\alpha_t} & l_3^2 C_{\alpha_t} \end{bmatrix}$$

K is the stiffness matrix,

$$K = 2\begin{bmatrix} 0 & 0 & -C_{\alpha_f} \\ 0 & 0 & (l_3 + d_1)C_{\alpha_t} \\ 0 & 0 & l_3 C_{\alpha_t} \end{bmatrix}$$

and F is given as:

$$F = 2C_{\alpha_f}\begin{bmatrix} 1 & l_1 & 0 \end{bmatrix}^T$$

Assuming that ε_f is very small, we have $\cos\varepsilon_f \approx 1$ and $\sin\varepsilon_f \approx \varepsilon_f$. Thus the nonlinear model represented by (2-7) becomes

$$\overline{M}\ddot{q} + \overline{D}\dot{q} + Kq = F\theta_w \tag{C-2}$$

where

$$\overline{M} = \begin{bmatrix} m_1 + m_2 & -m_2(d_1 + d_3) & -m_2 d_3 \\ -m_2(d_1 + d_3) & I_{z1} + I_{z2} + m_2(d_1{}^2 + d_3{}^2) + 2m_2 d_1 d_3 & I_{z2} + m_2 d_3{}^2 + m_2 d_1 d_3 \\ -m_2 d_3 & I_{z2} + m_2 d_3{}^2 + m_2 d_1 d_3 & I_{z2} + m_2 d_3{}^2 \end{bmatrix}$$

$$\overline{D} = D + \begin{bmatrix} 0 & (m_1 + m_2)\dot{x}_u & 0 \\ 0 & -m_2(d_1 + d_3)\dot{x}_u & 0 \\ 0 & -m_2 d_3 \dot{x}_u & 0 \end{bmatrix}$$

In fact, y_u has no explicit physical meaning since it is the lateral displacement of tractor CG with respect to the unsprung mass coordinate. Controlling ε_1, yaw angle of the tractor with respect to the inertial frame, makes no sense either. Since in lateral, we are interested in the lateral displacement of the vehicle with respect to the road centerline, the road reference frame is introduced to describe the tracking errors. The transformations from the former unsprung mass reference frame to the road reference frame is described as

$$\begin{cases} \dot{y}_u = \dot{y}_r - \dot{x}_r \varepsilon_r \\ \ddot{y}_u = \ddot{y}_r - \dot{x}_r \dot{\varepsilon}_r \\ \dot{\varepsilon}_1 = \dot{\varepsilon}_r + \dot{\varepsilon}_d \\ \ddot{\varepsilon}_1 = \ddot{\varepsilon}_r + \ddot{\varepsilon}_d \end{cases} \tag{C-3}$$

Therefore, the linearized HDV model with respect to the road reference frame is obtained as

$$\overline{M}\ddot{q}_r + D\dot{q}_r + \overline{K}q_r = F\theta_w + E_1\dot{\varepsilon}_d + E_2\ddot{\varepsilon}_d \tag{C-4}$$

where

$$q_r = \begin{bmatrix} y_r & \varepsilon_r & \varepsilon_f \end{bmatrix}^T$$

$$\overline{K} = 2\begin{bmatrix} 0 & -\left(C_{\alpha_f} + C_{\alpha_r} + C_{\alpha_t}\right) & -C_{\alpha_f} \\ 0 & -\left(l_1 C_{\alpha_f} - l_2 C_{\alpha_r} - (l_3 + d_1)C_{\alpha_t}\right) & (l_3 + d_1)C_{\alpha_t} \\ 0 & l_3 C_{\alpha_t} & l_3 C_{\alpha_t} \end{bmatrix}$$

$$E_1 = \begin{bmatrix} -\frac{2}{\dot{x}_u}\left(l_1 C_{\alpha_f} - l_2 C_{\alpha_r} - (l_3 + d_1)C_{\alpha_t}\right) - (m_1 + m_2)\dot{x}_u \\ -\frac{2}{\dot{x}_u}\left(l_1{}^2 C_{\alpha_f} + l_2{}^2 C_{\alpha_r} + (l_3 + d_1)^2 C_{\alpha_t}\right) + m_2(d_1 + d_3)\dot{x}_u \\ -\frac{2}{\dot{x}_u}\left(l_3(l_3 + d_1)C_{\alpha_t}\right) + m_2 d_3 \dot{x}_u \end{bmatrix}$$

$$E_2 = \begin{bmatrix} m_2(d_1 + d_3) \\ -\left(I_{z1} + I_{z2} + m_2(d_1{}^2 + d_3{}^2) + 2m_2 d_1 d_3\right) \\ -\left(I_{z2} + m_2 d_3{}^2 + m_2 d_1 d_3\right) \end{bmatrix}$$

(C-4) represents a linear model, whose outputs have physical meaning. The control input in this model is the front wheel angle θ_w, and $\dot{\varepsilon}_d$ and $\ddot{\varepsilon}_d$ are considered as input disturbances if they are small. If $\dot{\varepsilon}_d$ and $\ddot{\varepsilon}_d$ are too large to be neglected, we must take them into account in the control design. Note that the trailer mass m_2, longitudinal velocity $\dot{x}_u$ and road adhesion coefficient μ in the model may vary in practical applications, which will cause model uncertainties. More details the lateral truck model can be found in [18].

APPENDIX D: Sensors, Communication and Navigation for Truck Automation

D.1 On-board Sensors

To realize the developed longitudinal and lateral controllers, the essential measurements for feedback are the longitudinal velocity for each truck, relative distance and velocity between two adjacent trucks, and the lateral error at the point that is d_s ahead of the tractor CG. The truck velocity can be directly obtained by the speed sensor on board of the truck. A more precise way to obtain truck velocity is to install tachometers on different wheels, and calculate the truck velocity using the wheels velocities. To get the relative velocity, the supervisory controller needs only to calculate the difference of two velocities that are obtained by on-board tachometers. The relative distance can be detected by some video sensing systems that are used in the CHAUFFEUR project [4]. Another way to measure the relative distance and velocity is to employ a radar system, such as EVT-300, Eaton VORAD, which is currently used in PATH. It operates at 24.725GHz with the maximum power output of less than 5mW. It can detect different objects within its 12° radar beam with a range up to 350 feet. The system accuracy is 5% or ± 3 feet for the range and 1% or ± 0.2 mph for the relative velocity. However, when the follower tracks the leading truck "perfectly", i.e. the relative velocity is zero, the radar range drops down to zero due to the Doppler effect. Therefore, a robust compensator should be designed to filter the radar signal so that the relative distance does not drop to zero in the perfect tracking case.

The lateral error at the point d_s ahead of the tractor CG may not be obtained directly by sensors if that point is outside the truck and no sensor can be installed. California PATH has solved this problem by adopting a magnetic marker based road reference scheme. A series of magnets is embedded in the pavement along the road centerline and separated by about one meter distance. Arrays of five magnetometers are installed at the front and the rear ends of the tractor. The current scheme, based on look-up tables of magnetic field due to magnetic markers, provides accuracy of 1-2cm. The magnetometers have a sensing range of 0.8m on either side of the lane centerline. The lateral errors at the two independent arrays can be extended to obtain the "virtual error" at a point d_s ahead of the tractor CG. Preview of road curvature can also be encoded into the scheme by alternating the polarity of the magnets at special positions. An additional array of magnetometers should also be installed at the end of the trailer, so that the lateral error at the trailer end can be observed to evaluate the controller performance.

Other sensors, such as the steering and road wheel angle sensors, articulation angle sensors, accelerometers and gyroscopes, should also be installed to achieve a better control or observation of the truck behavior.

D.2 Radio Frequency Data Communication (RFDC)

RFDC can be used to provide direct real-time communications between the central computer and on-yard equipments. When any equipment in the yard changed its status, it transmits the new data via the nearest base station to the host computer. The central computer verifies the accuracy of this information updates the database and thus generates new real-time commands to the corresponding yard equipment(s). In the platoon case, RFDC can also be used to broadcast the leading truck's velocity or acceleration to its followers, so that the whole platoon can get better performance. There are two systems currently used for RFDC applications: narrow band and spread spectrum.

The narrow band system operates in the range of 400 to 512 MHz and transmits data at up to 10,000 bits per second (bps). This system needs the highest power (2 watts) among RFDC technologies and is able to transmit data over 1,000 to 5,000 feet. A Federal Communications Commission (FCC) site license is required to ensure that no other system within range operates on the assigned frequency. It is a good candidate for communication between on-yard equipment and the central computer, since the overall system cost is lower than other types of RFDC due to less costly components and fewer required base stations.

In the spread spectrum system, signals are transmitted over a wideband frequency: 900MHz or 2.4GHz. The spread spectrum of 902-928 MHz has intermediate range (approx. 135-300 m), moderate power (0.25-1 Watt), and high data transfer rates (60-600 Kbps). No site license is required. This range of frequency is available only in North America and Australia. The spread spectrum of 2.4-2.5 GHz is designed to offer transportability not only between facilities within North America but globally. They have the shortest range of all RFDC systems (approx. 75-210 m), least power (0.1 Watt), and highest data transfer rates (approx. 500 Kbps-2 Mbps). They do not require site licenses and this band is, or will be, available in most countries. In the CHAUFFEUR project [4], a spread spectrum system of 2.4GHz is used to broadcast the leading truck's information to its followers. In its potential follow-up project, it is planned to investigate the employment of a 5.8 GHz module.

D.3 Navigation Systems

The navigation system provides guidance and navigation to the AGV in the operating environment. The guidance and navigation could be based on a fixed-path or free-path approach [2]. In the fixed-path approach, the AGV is restricted to follow a fixed path and there is no flexibility to change the guide-path. In the free-path method, the path that an automated truck should follow can be changed dynamically according to the task requirement, traffic condition and other information. The system is autonomous and capable of detecting the path using online information, obstacle detection and collision avoidance systems.

In the proposed ACTIPOT system, the navigation system should at least have the following properties: high positional accuracy, fail-safe operations and all weather capability.

In the Delta Port of Rotterdam, the navigation system is designed by Free Ranging On Grid (FROG) Systems of the Netherlands, which utilizes fiber optic line grids and transponders located throughout the facility for position update information. Between transponders, the vehicles use their onboard inertial navigation system [2]. The fiber optic cables are embedded in a grid 20 centimeters below the ground. The primary drawback to the grid system is the transponder installation. At Rotterdam, this was not a serious problem since the system was installed during facility construction and the pavement surface is brick, which provides a dimensionally stable surface for embedding the transponders. In other existing ports, constructing such a system may not be feasible at all.

In nowadays technology, the Differential Global Positioning System (DGPS) system is able to serve as a navigation system for automated trucks. DGPS is robust and accurate up to ± 5 cm, has a relatively low cost installation, and requires few modifications to an area [11]. Every vehicle with a GPS receiver could be located precisely. To improve the reliability, vehicle-based DGPS can be coupled with an Inertial Measurement Unit (IMU) that provides continuous and precise vehicle movement data whenever the DGPS position signal is not available.

In case of the system failure, a second guidance system should be incorporated to supplement the primary navigation system. An approach, successfully implemented in Thamesport, utilizes a rotating Millimeter Wave Radar (MMWR) beam to locate itself by received reflections from passive reflectors mounted as know pointes in the operating area[11].

REFERENCES:

[1] Bose A. and Ioannou P., *"Analysis of Traffic Flow With Mixed Manual and Intelligent Cruise Control Vehicles: Theory and Experiments"*, California PATH Program, UCB-ITS-PRR-2001-13, 2001.

[2] Ioannou P., et al., *"Advanced Material Handling: Automated Guided Vehicles in Agile Ports"*, Technical Report, Center for Advanced Transportation Technologies, University of Southern California, October 2000.

[3] Hingwe P., Wang J., Tai M. and Tomizuka M., *"Lateral Control of Heavy Duty Vehicles for Automated Highway System: Experimental Study on a Tractor Semi-trailer"*, California PATH Program, UCB-ITS-PWP-2000-01, 2000.

[4] Schulze M., *"Promote-Chauffeur"*, final report TR1009, Chauffeur, DaimlerChrysler, 1999.

[5] Kelly T., *"Keeping Trucks on Track"*, ITS World, pp. 20-21, July/August 1999.

[6] Parker J.G., *"Trucks in a Row"*, Traffic World, pp. 23, July 12, 1999.

[7] ERTICO-ITS Europe, 1999.

[8] Tai M., Wang J., Hingwe P., Chen C. and Tomizuka M., *"Lateral Control of Heavy Duty Vehicles for Automated Highway Systems"*, California PATH Program, UCB-ITS-PRR-98-8, 1998.

[9] Yanakiev D. and Kanellakopoulos I., *"Analysis, Design, and Evaluation of AVCS for Heavy-Duty Vehicles with Actuator Delays"*, California PATH Program, UCB-ITS-PRR-98-18, 1998.

[10] Bose A. and Ioannou P., *"Evaluation of Mixed Automated/Manual Traffic"*, final Report for PATH MOU#290, September 1997.

[11] Larsen R., and Moses J., *"AVCS for Ports: An automation study for Norfolk International Terminals."* Working Paper, 1997.

[12] Swaroop D. and Hendrick J.K., *"String Stability of Interconnected Systems"*, IEEE Trans. on Automatic Control, vol. 41, No. 3, pp. 349-357, 1996.

[13] Yanakiev D. and Kanellakopoulos I., *"Engine and Transmission Modeling for Heavy-Duty Vehicles"*, California PATH Program, PATH Technical Note 95-6, 1995.

[14] Yanakiev D. and Kanellakopoulos I., *"Variable time Headway for String Stability of Automated Heavy-Duty Vehicles"*, Proc. of the 34th Conf. On Decision and Control, pp. 4077-4081, 1995.

[15] Shladover S., *"Review of the State of Development of Advanced Vehicle Control Systems (AVCS)"*, Vehicle System Dynamics, Swets & Zeitlinger, 24, pp. 551-595, 1995.

[16] Shladover, S., *"Longitudinal Control of Automated Guideway Transit vehicles within Platoons"*, ASME Journal of Dynamic Systems, Measurement, and Control, 100 (1978), pp. 302-310, 1995.

[17] Bareket Z. and Fancher P., *"Headway Control Systems and The Heavy Commercial Vehicle- A case Study"*, Road Transport Technology, No. 4, Univ. of Michigan Transp. Research Institute, 1995.

[18] Chen C., Tomizuka M., *"Dynamic Modeling of Tractor-Semitrailer Vehicles in Automated Highway Systems"*, UCB-ITS-PWP-95-8, July 1995.

[19] Chen C. and Tomizuka M., *"Steering and Braking Control of Tractor-Semitrailer Vehicles in Automated Highway Systems"*, Proc. of American Control Conference, pp. 658-662, 1995.

[20] URL: http://www.stt-ctt.nl/combi-road

[21] Chien C. and Ioannou P., *"Automatic Vehicle Following"*, Proc. of American Control Conference, pp. 1748-1752, 1992.

[22] McFarlane D. and Glover K., *"Robust Control Design Using Normalized Coprime Factor Plant Description"*, vol. 138 of "*Lecture Notes in Control and Information Sciences*", Spring-Verlag, 1990.

[23] Murata T., *"Petri Nets: Properties, Analysis and Applications"*, Proceedings of the IEEE, vol. 77, No 4, pp. 541-579, April 1989.